UHASSELT
KNOWLEDGE IN ACTION

Maastricht University

Faculty of Medicine and Life Sciences
School for Life Sciences
Master of Biomedical Sciences

Master's thesis

Hypertensive disorders of pregnancy as prenatal exposure on the morphology and functionality of the childhood microvasculature

Janne Pauwels

Thesis presented in fulfillment of the requirements for the degree of Master of Biomedical Sciences, specialization Environmental Health Sciences

SUPERVISOR :

Prof. dr. Michelle PLUSQUIN

MENTOR :

Mevrouw Hanne SLEURS

2021
2022

Transnational University Limburg is a unique collaboration of two universities in two countries: the University of Hasselt and Maastricht University.

UHASSELT
KNOWLEDGE IN ACTION

www.uhasselt.be
Universiteit Hasselt
Campus Hasselt:
Martelarenlaan 42 | 3500 Hasselt
Campus Diepenbeek:
Agoralaan Gebouw D | 3590 Diepenbeek

Maastricht University

Faculty of Medicine and Life Sciences
School for Life Sciences
Master of Biomedical Sciences

Master's thesis

Hypertensive disorders of pregnancy as prenatal exposure on the morphology and functionality of the childhood microvasculature

Janne Pauwels

Thesis presented in fulfillment of the requirements for the degree of Master of Biomedical Sciences, specialization Environmental Health Sciences

SUPERVISOR :

Prof. dr. Michelle PLUSQUIN

MENTOR :

Mevrouw Hanne SLEURS

Hypertensive disorders of pregnancy as prenatal exposure on the morphology and functionality of the childhood microvasculature*

Janne Pauwels[1], Hanne Sleurs[1], and Michelle Plusquin[1]

[1]Environmental Biology, Centre for Environmental Sciences (CMK), Hasselt University, Campus Diepenbeek, Agoralaan Gebouw D - B-3590 Diepenbeek

*Running title: *Exposure to hypertensive disorders of pregnancy*

To whom correspondence should be addressed: Prof dr. Michelle Plusquin, Tel: +32 (11) 26 82 89; Email: michelle.plusquin@uhasselt.be

Keywords: Hypertensive disorders of pregnancy, Prenatal exposure, Childhood microvasculature, Retinal vessels, Skin perfusion

ABSTRACT

One in ten pregnant women worldwide develops a hypertensive disorder of pregnancy (HDP), classified into four groups: *i.e.* essential hypertension, gestational hypertension, early-onset or late-onset pre-eclampsia. The offspring experience direct adverse effects from this prenatal exposure; however, long-term consequences related to the child's microvasculature are largely unknown. Therefore, this study investigated the effect of HDP on the microvascular health of 4 to 6-year-old children. Morphology and functionality of the small blood vessels in the retina and skin were examined. Morphology was determined by retinal photography and software analysis of the retinal vessel nature. Functionality was investigated by heat-controlled provocation of the skin during blood flow measurements with laser Doppler technology. In a case-control and case-cohort design with matching of child's age and sex, a comparison was made between children exposed and non-exposed to HDP. Furthermore, differences in the four HDP categories were studied, compared to no exposure. Linear regression and mixed effect models, adjusted for relevant covariates, were applied. Exposure to HDP, mainly driven by gestational hypertension, was associated with narrower retinal arterioles, and exposure to early-onset pre-eclampsia with decreased tortuosity. Furthermore, exposure to HDP, mainly driven by early-onset pre-eclampsia, was positively associated with the vasodilatory response. These findings implicate that the altered microvascular phenotype might form a link between HDP exposure and childhood hypertension with future cardiovascular disease onset. The increased vasodilatory function might be a compensatory response of the vessels after exposure to HDP. More investigation into the related mechanisms and follow-up of the children is recommended.

INTRODUCTION

Worldwide, 10% of all pregnant women develop hypertensive disorders of pregnancy (HDP) (1, 2). These disorders are characterized by high blood pressure during pregnancy, with a systolic blood pressure (SBP) of 140 mmHg or more and/or a diastolic blood pressure (DBP) of 90 mmHg or more (2, 3). HDP contributes to the leading cause of maternal, fetal and neonatal morbidity and mortality with a significant economic impact on the health care system (2, 4). Furthermore, risk factors of HDP development, such as chronic hypertension, high body mass index (BMI) and type 2 diabetes mellitus, are more common nowadays (3, 5).

During pregnancy, the maternal body undergoes many physiological changes to ensure adequate blood flow through the placenta to the growing fetus (3, 6, 7). On the one hand, vascular and renal adaptations occur: the maternal cardiac output rises

30 to 50% above baseline, the peripheral vascular resistance changes, vasodilation of the blood vessels occurs, and the erythrocyte production and body fluid volume increases (3, 6). Additionally, metabolic and immune responses appear, such as hormone secretion by the placenta to alter lipid and glucose metabolism and upregulation of the pancreatic function, to counter the demands of the growing fetus (3). All these adaptations are essential to provide the fetus with sufficient nutrients and oxygen; however, dysregulation may manifest with HDP development (7).

There exist four significant categories of HDP (**Fig. 1**). The first one is essential or chronic hypertension (EH), referred to as the presence or history of maternal high blood pressure preconceptionally or before 20 weeks of pregnancy (2). This group of women is estimated to be 1-5% of all pregnancies (8). The second category is gestational hypertension (GH); a high blood pressure condition developed *de novo* in previously normotensive pregnant women at 20 weeks or more of gestation (2, 3). This disorder occurs in 3-14% of pregnancies worldwide (3). The third and the fourth group include early-onset and late-onset pre-eclampsia (7), (9). Pre-eclampsia is a condition of high blood pressure and the presence of at least one of the following signs of end-organ dysfunction: proteinuria (300 mg or more proteins in a 24-hour urine collection or 1+ on the urine dipstick reading), thrombocytopenia (platelet count less than $100*10^9$/L), renal insufficiency (creatinine more than 1.1 mg/dL urine), impaired liver function (transaminases elevated twice as normal), pulmonary edema, or cerebral and visual symptoms (1-3). This condition appears in 3-5% of all pregnancies (1, 3). Pre-eclampsia is indicated as early-onset when the clinical presentation starts at less than 34 weeks of pregnancy, and this group comprises 25% of the pre-eclamptic pregnancies (3, 7). Early-onset pre-eclampsia (EPE) is associated with poor early placentation, and is, therefore, known as placental pre-eclampsia (10, 11). In addition, pre-eclampsia is indicated as late-onset when it starts at 34 weeks or more, which has a prevalence of 75% within the pre-eclampsia group (3, 7). Late-onset pre-eclampsia (LPE) has potential origins derived from maternal exaggerated systemic inflammatory responses with uteroplacental malperfusion, and is therefore considered as maternal pre-eclampsia (10, 11). However, the division of placental and maternal pre-eclampsia is rather a hypothesis and a revised two-stage placental model (2019) is recently suggested (12). This model describes the two main placental pathways to clinical pre-eclampsia (stage 1: placental dysfunction; stage 2: maternal clinical syndrome), which may be both affected by maternal risk factors, such as chronic arterial disease, obesity, and some auto-immune diseases (12). Besides the difference in onset during pregnancy, a significant contrast between the two types of pre-eclampsia is the severity of the organ dysfunctions; higher severity in early-onset than in late-onset pre-eclampsia (13).

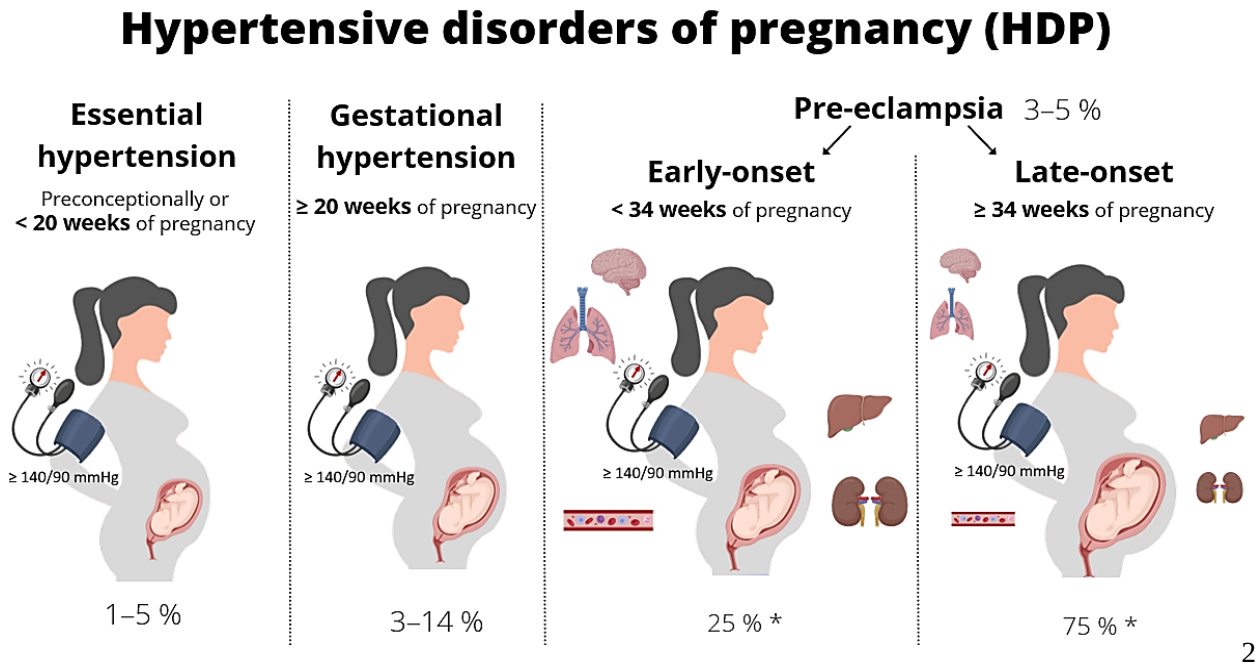

Fig. 1: Overview of the four categories of hypertensive disorders of pregnancy (HDP). These disorders are characterized by a systolic blood pressure of 140 mmHg or more and/or a diastolic blood pressure of 90 mmHg or more, all with a clinical presentation at a different timepoint in pregnancy. Additionally, in pre-eclampsia (both early-onset and late-onset) organ dysfunction occurs, such as renal failure, impaired liver function, thrombocytopenia, pulmonary edema, or cerebral and visual symptoms. The symptoms are more severe in early-onset pre-eclampsia. Prevalence per group in all pregnancies worldwide is given.
* = prevalence within the pre-eclampsia group

HDP have a significant impact on maternal health in the immediate and long term (1). Several studies have shown increased risks for future metabolic, cardiovascular and renal diseases such as stroke, hypertension and diabetes (3, 14-16). Benschop *et al.* (Generation R Study) have demonstrated an altered status of the maternal microvasculature, investigated by retinal photography, 6 years after HDP, suggesting that microvascular changes may form a link between HDP and the development of cardiovascular diseases (CVDs) later in life (15).

Furthermore, HDP also negatively affects the fetus: immediate adverse outcomes include intrauterine growth restriction (IUGR), preterm birth (both spontaneous and iatrogenic), oligohydramnios, placental abruption, fetal distress, and fetal death *in utero* (1). Early-onset pre-eclampsia has been associated with significantly higher rates of these adverse outcomes (1, 3, 7). In addition, long-term effects on the offspring are observed (1). According to the Barker or DOHaD hypothesis, health and disease have a developmental origin (17). This principle states that adverse influences and exposures during the intrauterine life can predispose the fetus to develop diseases later in life, such as CVDs (3, 18). Therefore, HDP and the general maternal cardiovascular health may also affect the child (19). In this regard, research has revealed elevated blood pressure levels in 3 to 18-year-old children exposed to HDP (20, 21). Furthermore, Hammad *et al.* have shown increased overall mortality risks in 49 to 69-year-old adults born from hypertensive disordered pregnancies (22). Moreover, Huang *et al.* has observed that exposure to HDP was associated with an increased risk for early-onset CVD onset from birth to young adulthood (up to 40 years old) (23).

The microvasculature or microcirculation consists of the smallest blood vessels in the human body with diameters ranging from 5 – 400 µm, which form the terminal vascular network of the systemic circulation (24, 25). These refined microvascular vessels (arterioles, capillaries and venules) provide oxygen and nutrient exchange with organs (**Fig. 2**) (25, 26). Because of their small size, they are one of the first compartments affected during the development of hypertension (27, 28). Furthermore, the microvasculature undergoes extensive, organ-specific prenatal maturation, which may make it more sensitive to prenatal exposures (29-31). Accordingly, the condition of the microvasculature can indicate the risk of hypertension and CVDs in adults (32), because it also controls the peripheral vascular resistance to regulate capillary exchange (32, 33). When the microvasculature is affected and remodeling with reduction of the vessel lumen occurs, the systemic vascular resistance can elevate (34). This can subsequently lead to hypertension and CVD development (34). Therefore, microvascular dysfunction is both a cause and consequence of elevated blood pressure (32).

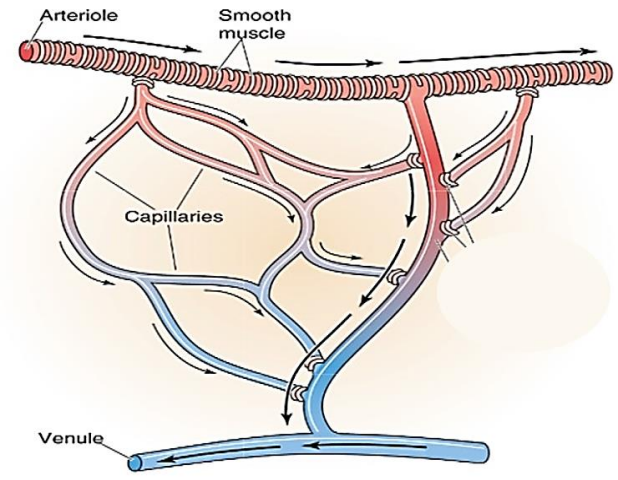

Fig. 2: The microcirculation or microvasculature, shown within a smooth muscle. It consists of three types of small vessels: arterioles, capillaries and venules. (25)

The microvascular vessels from the eye, also called the retinal microvasculature, offer a direct non-invasive visualization of the entire human microcirculation, as they share similar characteristics as other microvascular vessels of, for example, the brain and kidney (28). Retinal vessel diameters range from 150 – 300 µm (35). With retinal photography, the retinal vessel nature (vessel calibers and tortuosity), and thus the

morphology of the microvasculature can be examined (28, 32). These parameters can give an indication of the cardiovascular health (27, 28); *e.g.* retinal arteriolar narrowing and venular widening in adults is shown to be independently associated with an increased risk of hypertension and CVD (35, 36).

In addition, the microvascular vessels from the skin, also called the skin microvasculature, can provide a non-invasive determination of the functionality of the microvasculature (30, 37). Endothelial cell dysfunction plays an essential role in the development and progression of CVDs (30). A prominent function of the microvascular endothelium is to regulate perfusion within organ tissues (25). The endothelium releases vasodilating (*i.e.* nitric oxide (NO)) and vasoconstricting (*i.e.* endothelin) factors to control the blood flow during, for example, temperature changes (30). In this regard, skin perfusion can serve as a dynamic marker of the endothelial microvascular function.

Because the microvascular phenotype plays a role in hypertension and CVD development, it might form a link between HDP exposure and childhood hypertension with future CVD onset. In this regard, the Generation R study (Yesil *et al.*, 2016) investigated the morphology of the childhood microvasculature with retinal photography and revealed narrowing of the retinal arterioles in 6-year-old children exposed to HDP in Rotterdam (the Netherlands) (38). Knowledge about the effects of HDP on the functionality of the offspring's blood vessels is largely missing.

Therefore, this study compared results of retinal vessel nature and skin perfusion of children exposed to HDP with those non-exposed, to gather more insights into the effects of HDP on the microvascular morphology and functionality, respectively. Furthermore, a comparison was made concerning the four different HDP categories and non-HDP, to differentiate more at-risk offspring with a view to future investigation into the mechanisms of HDP effects. It was hypothesized that prenatal exposure to HDP negatively affects both the child's microvascular morphology and functionality, as a possible link between HDP exposure and childhood hypertension with future CVD risks. In addition, early-onset pre-eclampsia and gestational hypertension were hypothesized to be associated with more prominent effects in the offspring, based on the severity of maternal symptoms, and on the exposure length and maternal novelty to high blood pressure, respectively.

EXPERIMENTAL PROCEDURES

Study design & participant recruitment – This research was embedded in the CArdioVAscular (CAVA) study of Hasselt University as part of the ENVIR*ON*AGE (ENVIRonmental influence *ON* early AGEing) birth cohort, in collaboration with Hospital East-Limburg in Genk (Belgium). The followed procedure within ENVIR*ON*AGE, an ongoing population-based cohort, is described in detail elsewhere (39). Since May 2016, the hemodynamics of pregnant women with hypertension (SBP $\geq$ 140 mmHg and/or DBP $\geq$ 90 mmHg) were investigated within the "Limburgs Pre-eclampsia Onderzoek" (LimPrOn) study for early diagnosis of HDP (40). Mothers diagnosed with HDP were contacted after 4 – 6 years to participate with their children in the CAVA study for follow-up of their current (vascular) health condition. Twin pregnancies and cases of fetal or pediatric death were excluded. As similar follow-up measurements were performed in both the CAVA and ENVIR*ON*AGE study, a case-control/case-cohort design (CAVA or HDP *versus* ENVIR*ON*AGE or non-HDP) could be applied within the current study. Participants with hypertension and pre-eclampsia were excluded from the ENVIR*ON*AGE population. All follow-up examinations of the HDP group (October 2018 – May 2022) and most of the non-HDP group (October 2014 – December 2021) were performed at Hasselt University campus Diepenbeek (Belgium), whereby the skin perfusion measurements of the non-HDP group were obtained during house visits (April 2017 – April 2018) (30). All procedures of recruitment and follow-up examination are approved by the Ethical Committee of Hasselt University and Hospital East-Limburg, and conducted according to the principles of the Helsinki declaration (41). Written informed consent was obtained from the parents and oral assent from the child during the follow-up examination. Detailed health and lifestyle data of mother and child were obtained by questionnaires. Information on pregnancy outcomes and pre-pregnancy BMI was obtained from the medical files collected in the hospital. In total, 69 mother-child pairs were recruited for the HDP group. After

exclusion of statistical outliers for the outcome variables (threshold of 3 times the standard deviation (SD) of the mean) and missings in mean arterial pressure (MAP), participants with retinal microvascular data (n = 63) were matched in a case-control design (ratio 1:2) with the non-HDP group (n = 423) based on optimal pair matching of child's sex and age (**Fig. S1**)**.** Participants with skin microvascular data (n = 50) were matched in a case-cohort design with the non-HDP group (n = 125) based on constrained full matching of child's sex and age (**Fig. S1**). Matching balance was evaluated and reported with Love plots, density plots and summary tables (**Fig. S2, Fig. S3**).

Clinical measurements & data analysis – Morphology of the childhood microvasculature was determined by retinal photography with the Canon CR2-plus 45° digital nonmydriatic retinal camera (Hospithera, Brussels, Belgium), which consisted out of four different pixel resolutions throughout the years of follow-up examination. Fundus pictures of the child's both eyes were taken according to the manufacturer's protocol (42). Hereafter, photographs were analyzed with the MONA-REVA software (version 3.0.0, VITO Health, Mol, Belgium) to determine the retinal microvascular calibers and tortuosity index (TI). Average values of the child's both eyes were used, if both pictures were available and of sufficient quality (n_{HDP} = 56; $n_{non\text{-}HDP}$ = 105). Otherwise, only the picture of one eye was used (n_{HDP} = 7; $n_{non\text{-}HDP}$ = 21). Analyses were performed by a single trained examiner with correction for the different pixel resolutions. First, the diameter of the optic disk (OD) was determined for each picture, since all distance measurements within the fundus were set relative to this value. Next, the retinal vessel calibers were obtained by determining the diameters of the six largest arterioles and six largest venules, within the area of 0.5 to 1 times the OD diameter starting from its margin, to subsequently calculate the central retinal arteriolar equivalent (CRAE) and central retinal venular equivalent (CRVE) with the revised Parr-Hubbard formula (29) (**Fig. S4 A**). CRAE is considered as the average arteriolar diameter and CRVE as the average venular diameter. The TI, representing the curvature of retinal vessels as the ratio between the length along the centerline of the vessel and the linear distance between the two endpoints, was determined between 1.5 and 5 times the radius of the OD (**Fig. S4 B**). Batch effect of the four camera resolutions was evaluated by overlap density plots and one-way ANOVA tests (**Fig. S5**).

Functionality of the microvasculature was determined by thermal provocation of the skin during blood flow measurements by a laser Doppler system (Periflux 6000, Perimed, Stockholm, Sweden). Two thermostatic laser Doppler probes (PROBE 457 Thermostatic Small-Angled Probe, Perimed) were attached to the child's chest with double-sided tape (PF 105-3 Double-Sided Tape Strips, Perimed). Before applying the probes, alcohol tissues (Soft-Zellin, Hartmann, 70% alcohol) were used to clean the places on the chest. These places were located directly under the left and right nipple with avoidance of bony prominences, areas of edema, large superficial vessels, callused skin, and infected or inflamed areas (**Fig. S6 A**). The thermostatic probes can simultaneously detect blood flow changes according to the Doppler phenomenon and locally heat the skin (43). The probes emit a low-power laser light beam (780 nm), with a known frequency (*i.e.* 32 Hz), which is scattered by moving red blood cells in the skin vessels, represented as the Doppler shift. This shift has a frequency and size associated with the velocity and concentration of the red blood cells, respectively (30, 44). Therefore, information of the returning light signals is picked up by the probes and converted into an electric signal on the device to analyze the blood flow in arbitrary perfusion units (PU; *i.e.* the product of the velocity and concentration of moving red blood cells) (37, 45) **(Fig. S6 B)**. The laser-Doppler output was recorded for at least 17 minutes, while the child was quietly sitting in an upright position and watching television. After a baseline perfusion measurement for 2 minutes (unheated), one probe (right) was rapidly and locally heated to 42°C, while the other probe (left) continued to record blood flow changes at body temperature to serve as reference for quality control. Local heating of the skin to 42°C elicits maximal vasodilatation with a typical course of skin perfusion (PU) over time (min.) (**Fig. S6 C**). The heat-induced skin hyperemic response was expressed as the absolute difference of the average PU increase during stabilization in the 15-min heating phase and the average 2-min baseline phase (30). Average PU were calculated during the last 30 seconds of each phase. Graphical reports and

measurement data were visually controlled before inclusion into the study.

The MAP was calculated through the equation: MAP = (2/3 x DBP) + (1/3 x SBP). Both SBP and DBP were measured on the right upper-arm with an automated oscillometric blood pressure monitor (Omron 705IT, Omron Corporation, Japan), according to a standardized method (46). Average SBP and DBP values, used to determine the MAP, were calculated on the last three readings out of five consecutive readings with 1-min intervals.

Statistical analysis – All analyses were performed with the statistical software R (version 4.0.5 (2021.09.2+382)). Differences in participant characteristics between HDP and non-HDP, were tested by two-sided t-tests for continuous variables or Welch's t-tests when no homoscedasticity, and with chi-square tests and Wilcoxon rank-sum tests for nominal and ordinal variables, respectively. Characteristics differences between the four HDP categories and non-HDP were tested by one-way ANOVA tests for continuous variables or Kruskal-Wallis tests for non-parametrical and ordinal variables, and Fisher's exact tests for nominal variables. Correlations were examined by Pearson's correlation. Main models were created with adjustment of relevant covariates, selected *a priori* and complemented by the DAGitty program (**Fig. S7**). Assumptions for model linearity (normality, homoscedasticity, linearity and independence) were verified. Statistical significance was set at $p < 0.05$. Linear mixed effect models were used to analyze the association between exposure to one of the HDP groups or non-HDP and retinal microvascular outcome variables (CRAE, CRVE, TI), accounted for the batch effect of camera resolution. Associations were adjusted for child's sex, age, MAP, birthweight and BMI, mother's age, pre-pregnancy BMI and education, season of examination, and CRVE when CRAE was the dependent variable and vice versa. Linear regression models were used to analyze the association between exposure to one of the HDP groups or non-HDP and the skin hyperemic response data, which were naturally log-transformed to obtain better model linearity. Associations were adjusted for child's sex, age, MAP, birthweight and BMI, mother's age, pre-pregnancy BMI and education, and season of examination, start temperature and baseline value of the measurement. Furthermore, four sensitivity analyses were performed for all main models; *i.e.* adjustment for gestational age instead of birthweight to correct for prematurity, and additional adjustment for alcohol consumption, smoking during pregnancy, and year of follow-up examination. An overview can be found in **Fig. S8**.

RESULTS

Population characteristics – General characteristics of the entire HDP population (n = 69) compared to the entire non-HDP population (n = 549) were summarized in **Table S1**. General characteristics of the entire non-HDP population compared to the matched non-HDP population for the retinal (n = 126) and skin microvasculature (n = 125) were shown in **Table S2**.

Main characteristics of the HDP population with the four categories (*EH*: n = 6; *GH*: n = 17; *EPE*: n = 12; *LPE*: n = 28) and the total HDP group (n = 63), compared to the optimal pair matched non-HDP population (n = 126) for the retinal microvasculature, were summarized in **Table 1**. Of the children participating, 63.5 % and 59.5 % were girls in the HDP and non-HDP group, respectively. In general, the child's mean (SD) age (months) at time of follow-up examination was higher in the HDP population: ranging between 65.4 (7.62) and 66.9 (4.99) months within the four categories of HDP, and 66.1 (6.63) months in the total HDP group, compared to 60.8 (4.71) months in the non-HDP group ($p = 7.5*10^{-8}$ and $1.4*10^{-7}$, respectively). The MAP was higher in the HDP population, with a mean (SD) of 74.8 (7.64) mmHg in the total HDP group, compared to 71.4 (8.72) mmHg in the non-HDP group ($p = 0.007$). The child's birthweight was significantly different between the HDP and non-HDP population, with a mean (SD) of 2800 (918) grams for the total HDP group compared to 3380 (467) grams for the non-HDP group ($p = 9.4*10^{-6}$). Follow-up visits took place during all seasons.

Main characteristics of the HDP population with the four categories (*EH*: n = 3; *GH*: n = 14; *EPE*: n = 11; *LPE*: n = 22) and the total HDP group (n = 50), compared to the constrained full matched non-HDP population (n = 125) for the skin microvasculature, were summarized in **Table 2**.

Table 1: Main characteristics of the retinal microvascular population: the optimal pair matched non-HDP group, the four HDP categories and the total HDP group, expressed in mean (SD) or frequency (%). P-values were calculated to compare the four HDP categories with the non-HDP group and to compare the total HDP group with the non-HDP group, respectively.

	Retinal microvasculature: Case – control design							
Characteristic	**Non-HDP** *N = 126*	**Essential hypertension** *N = 6*	**Gestational hypertension** *N = 17*	**Early-onset pre-eclampsia** *N = 12*	**Late-onset pre-eclampsia** *N = 28*	**p-value**	**HDP (total)** *N = 63*	**p-value**
Mother								
Age at birth child (years)	29.8 (4.47)	31.6 (4.8)	30.9 (3.4)	31.6 (5.04)	30.8 (4.44)	0.44	31.1 (4.25)	0.06
Pre-pregnancy BMI (kg/m²)	24.6 (4.74)	27.3 (3.95)	24.5 (4.58)	27.3 (4.26)	23.7 (3.41)	0.04 [a]	24.9 (4.15)	0.67
Education level						0.17		0.03
Low (no high school diploma)	7 (5.6)	0 (0)	1 (5.9)	1 (8.3)	1 (3.6)		3 (4.8)	
Middle (high school diploma)	34 (27)	3 (50)	3 (17.6)	5 (41.7)	13 (46.4)		24 (38.1)	
High (college degree or higher)	85 (67.5)	3 (50)	13 (76.5)	6 (50)	14 (50)		36 (57.1)	
Child								
Sex						0.67		0.71
Male	51 (40.5)	3 (50)	8 (47.1)	3 (25)	9 (32.1)		23 (36.5)	
Female	75 (59.5)	3 (50)	9 (52.9)	9 (75)	19 (67.9)		40 (63.5)	
Age at examination (months)	60.8 (4.71)	65.4 (11.0)	66.9 (4.99)	66.7 (3.41)	65.4 (7.62)	$7*10^{-8}$ [a]	66.1 (6.63)	$1*10^{-7}$ [b]
Birthweight (grams)	3380 (467)	3430 (443)	3260 (522)	1260 (414)	3030 (575)	$< 2*10^{-16}$	2800 (918)	$9*10^{-6}$ [b]
BMI at examination (kg/m²)	16.2 (1.32)	16.5 (1.37)	15.8 (0.71)	15.4 (1.44)	16 (1.28)	0.13 [a]	15.8 (1.2)	0.10
MAP (mmHg)	71.4 (8.72)	76.8 (5.67)	74.6 (7.65)	75.1 (8.15)	74.3 (8.08)	0.007 [a]	74.8 (7.64)	0.007
Season at examination						0.31		0.12
Spring	50 (39.7)	1 (16.7)	4 (23.5)	5 (41.7)	14 (50)		24 (38.1)	
Summer	20 (15.9)	2 (33.3)	7 (41.2)	3 (25)	5 (17.9)		17 (27)	
Autumn	24 (19)	0 (0)	1 (5.9)	1 (8.3)	3 (10.7)		5 (7.9)	
Winter	32 (25.4)	3 (50)	5 (29.4)	3 (25)	6 (21.4)		17 (27)	

(non-)HDP = (non-)hypertensive disorders of pregnancy; MAP = mean arterial pressure; BMI = body mass index

[a] *P-values were obtained with a Kruskal-Wallis test instead of a one-way ANOVA test.*

[b] *P-values were obtained with a Welch's t-test instead of an unpaired t-test.*

Of the children participating, 66 % and 48 % were girls in the HDP and non-HDP group, respectively. In general, the child's mean (SD) age (months) at time of follow-up examination was higher in the HDP population: ranging between 66.7 (3.36) and 72.7 (8.18) months within the four HDP categories, and 67.5 (6) months in the total HDP group, compared to 57.8 (6.75) months in the non-HDP group ($p = 1.9*10^{-13}$ and $3.8*10^{-15}$, respectively). The MAP was higher in the HDP population, with a mean (SD) of 74.7 (8.47) mmHg in the total HDP group, compared to 69.7 (6.57) mmHg in the non-HDP group ($p = 4*10^{-4}$). The child's birthweight was significantly different between the HDP and non-HDP population, with a mean (SD) of 2740 (961) grams for the total HDP group compared to 3420 (477) grams for the non-HDP group ($p = 1*10^{-5}$). Follow-up visits for the HDP group took place during all seasons, for the non-HDP group only during spring and summer.

Microvascular characteristics – Values of CRAE, CRVE and TI in the right and left eye were highly correlated in both the HDP group (*CRAE*: $r = 0.71$, $p = 9.8*10^{-10}$; *CRVE*: $r = 0.67$, $p = 2.1*10^{-8}$; *TI*: $r = 0.78$, $p = 1.4*10^{-12}$) and non-HDP group (*CRAE*: $r = 0.6$, $p = 2.7*10^{-11}$; *CRVE*: $r = 0.63$, $p = 7.4*10^{-13}$; *TI*: $r = 0.5$, $p = 2*10^{-4}$). For the HDP population, the mean (SD) CRAE, CRVE and TI were 156 (14.5) µm, 226 (15.9) µm and 0.894 (0.0161), respectively (**Table 3**). The mean (SD) CRAE, CRVE and TI values for the non-HDP population were 172 (13.6) µm, 243 (18.7) µm and 0.894 (0.0114), respectively (**Table 3**). Within the four HDP categories, the mean (SD) for CRAE ranged between 151 (13.5) and 159 (14.5) µm, the CRVE between 220 (20.8) and 228 (14.1) µm, and the TI between 0.878 (0.0229) and 0.898 (0.0134) (**Table 3**). A positive correlation was found between CRAE and CRVE in both the HDP ($r = 0.65$, $p = 1.1*10^{-08}$) and non-HDP group ($r = 0.6$, $p = 9.4*10^{-12}$). The mean (SD) heat-induced skin

hyperemic response for the HDP group was 124 (43) PU based on the right probe, for non-HDP 112 (36.5) PU based on the average of the right and left probe (**Table 3**). Within the four categories of HDP, the mean (SD) heat-induced skin hyperemic response ranged between 117 (40.6) and 129 (50.2) PU (**Table 3**). The mean (SD) start temperature of the measurement for the HDP group was 31.6 (1.83) °C and for the non-HDP group 32.4 (0.923) °C (p = 0.0037). Mean baseline values (SD) for the HDP group were 24.5 (10.6) PU and 22.9 (13.0) PU for the non-HDP group (p = 0.4). Start temperatures and baseline values were correlated (r = 0.24, p = 0.001).

Table 2: Main characteristics of the skin microvascular population: the constrained full matched non-HDP group, the four HDP categories and the total HDP group, expressed in mean (SD) or frequency (%). P-values were calculated to compare the four HDP categories with the non-HDP group and to compare the total HDP group with the non-HDP group, respectively.

	Skin microvasculature: Case – cohort design							
Characteristic	**Non-HDP** *N = 125*	**Essential hypertension** *N = 3*	**Gestational hypertension** *N = 14*	**Early-onset pre-eclampsia** *N = 11*	**Late-onset pre-eclampsia** *N = 22*	**p-value**	**HDP (total)** *N = 50*	**p-value**
Mother								
Age at birth child (years)	30.8 (3.88)	31.9 (6.16)	30.3 (3.09)	31 (4.28)	31.2 (4.15)	0.94	30.9 (3.92)	0.78
Pre-pregnancy BMI (kg/m²)	23.4 (3.45)	28.7 (5.16)	24.9 (4.74)	26.9 (4.51)	23.4 (3.57)	0.03 [a]	24.9 (4.4)	0.04 [b]
Education level						0.11		0.03
Low (no high school diploma)	8 (4.6)	0 (0)	2 (14.3)	1 (9.1)	0 (0)		3 (6)	
Middle (high school diploma)	41 (23.4)	1 (33.3)	2 (14.3)	5 (45.5)	13 (59.1)		17 (34)	
High (college degree or higher)	126 (72)	2 (66.7)	10 (71.4)	5 (45.5)	9 (40.9)		30 (60)	
Child								
Sex						0.16		0.05
Male	65 (52)	1 (33.3)	6 (42.9)	2 (18.2)	8 (36.4)		17 (34)	
Female	60 (48)	2 (66.7)	8 (57.1)	9 (81.8)	14 (63.6)		33 (66)	
Age at examination (months)	57.8 (6.75)	72.7 (8.18)	67.8 (3.87)	66.7 (3.36)	66.9 (7.64)	$1.9*10^{-13}$	67.5 (6)	$3.8*10^{-15}$
Birth weight (grams)	3420 (477)	3300 (185)	3280 (528)	1260 (456)	3070 (616)	$< 2*10^{-16}$	2740 (961)	$1*10^{-5}$ [b]
BMI at examination (kg/m²)	15.9 (1.3)	16.2 (1.39)	15.8 (0.85)	15.3 (1.6)	16 (1.31)	0.35 [a]	15.8 (1.27)	0.54
MAP (mmHg)	69.7 (6.57)	77.4 (6.01)	74.6 (7.69)	73.7 (10.4)	74.8 (8.65)	0.001 [a]	74.7 (8.47)	$4*10^{-4}$ [b]
Season at examination						$4.9*10^{-8}$		$1.4*10^{-10}$
Spring	87 (69.6)	0 (0)	2 (14.3)	5 (45.5)	9 (40.9)		16 (32)	
Summer	38 (30.4)	2 (66.7)	6 (42.9)	4 (36.4)	6 (27.3)		18 (36)	
Autumn	0 (0)	0 (0)	1 (7.1)	0 (0)	1 (4.5)		2 (4)	
Winter	0 (0)	1 (33.3)	5 (35.7)	2 (18.2)	6 (27.3)		14 (28)	

(non-)HDP = (non-)hypertensive disorders of pregnancy; MAP = mean arterial pressure; BMI = body mass index

[a] *P-values were obtained with a Kruskal-Wallis test instead of a one-way ANOVA test.*

[b] *P-values were obtained with a Welch's t-test instead of an unpaired t-test.*

Table 3: Microvascular characteristics of the four HDP categories, the total HDP population and the non-HDP population, expressed in mean (SD).

	Essential hypertension	**Gestational hypertension**	**Early-onset pre-eclampsia**	**Late- onset pre-eclampsia**	**HDP (total)**	**Non-HDP**
Retinal microvasculature:	*N = 6*	*N = 17*	*N = 12*	*N = 28*	*N = 63*	*N = 126*
CRAE (µm)	152 (13.3)	155 (15.4)	151 (13.5)	159 (14.5)	156 (14.5)	172 (13.6)
CRVE (µm)	220 (20.8)	227 (19)	224 (13)	228 (14.1)	226 (15.9)	243 (18.7)
TI	0.898 (0.0134)	0.897 (0.0103)	0.878 (0.0229)	0.897 (0.0121)	0.894 (0.0161)	0.894 (0.0114)
Skin microvasculature:	*N = 3*	*N = 14*	*N = 11*	*N = 22*	*N = 50*	*N = 125*
Skin hyperemic response (PU)	122 (40.7)	117 (40.6)	129 (50.2)	126 (43.4)	124 (43)	112 (36.5)

(non-)HDP = (non-)hypertensive disorders of pregnancy; CRAE = central retinal arteriolar equivalent; CRVE = central retinal venular equivalent; TI = tortuosity index; PU = perfusion units

Main analyses

Retinal microvasculature – The main linear mixed effect model with the HDP and non-HDP group showed a negative association between HDP exposure and the CRAE value (µm) in childhood (β = -5.25; 95 % CI = -10.8 to -0.62; p = 0.04) (**Fig. 3**). More specifically, exposure to gestational hypertension was associated with significantly lower CRAE values compared to no exposure to HDP (β = -6.98; 95 % CI = -14.63 to -0.92; p = 0.04) (**Fig. 3**). Trends were found between exposure to HDP, or one of the four categories of HDP, compared to non-HDP, and lower CRVE values (µm) in childhood (β = -5.34; 95 % CI = -11.15 to 0.37; p = 0.09) (**Fig. 3**). There was no significant association between exposure to HDP and the TI (β = -0.0014; 95 % CI = -0.0068 to 0.0061; p = 0.6), compared to non-HDP (**Fig. 3**). More specific exposure to early-onset pre-eclampsia showed a lower TI value compared to no exposure to HDP (β = -0.028; 95 % CI = -0.039 to -0.013; p = $1.2*10^{-5}$) (**Fig. 3**).

Skin microvasculature – The main multiple linear regression model with the HDP and non-HDP group showed a positive association between HDP exposure and the heat-induced skin hyperemic response (expressed in %) in childhood (β = 25.73; 95 % CI = 5.02 to 50.68; p = 0.04) (**Fig. 4**). More specifically, exposure to early-onset pre-eclampsia (β = 49.8; 95 % CI = 4.95 to 113.83; p = 0.02) and essential hypertension (β = 69.2; 95 % CI = 15.14 to 148.43; p = 0.0495), compared to no HDP exposure, was associated with a significant higher heat-induced skin hyperemic response (**Fig. 4**).

No correlation or association was found between the retinal microvascular nature and the heat-induced skin hyperemic response within the HDP group.

Sensitivity analyses

The results of the sensitivity analyses for both retinal and skin microvasculature were summarized in **Table 4**.

Retinal microvasculature – Gestational age (weeks) and birthweight (grams) were highly correlated (r = 0.81, p < $2.2*10^{-16}$).

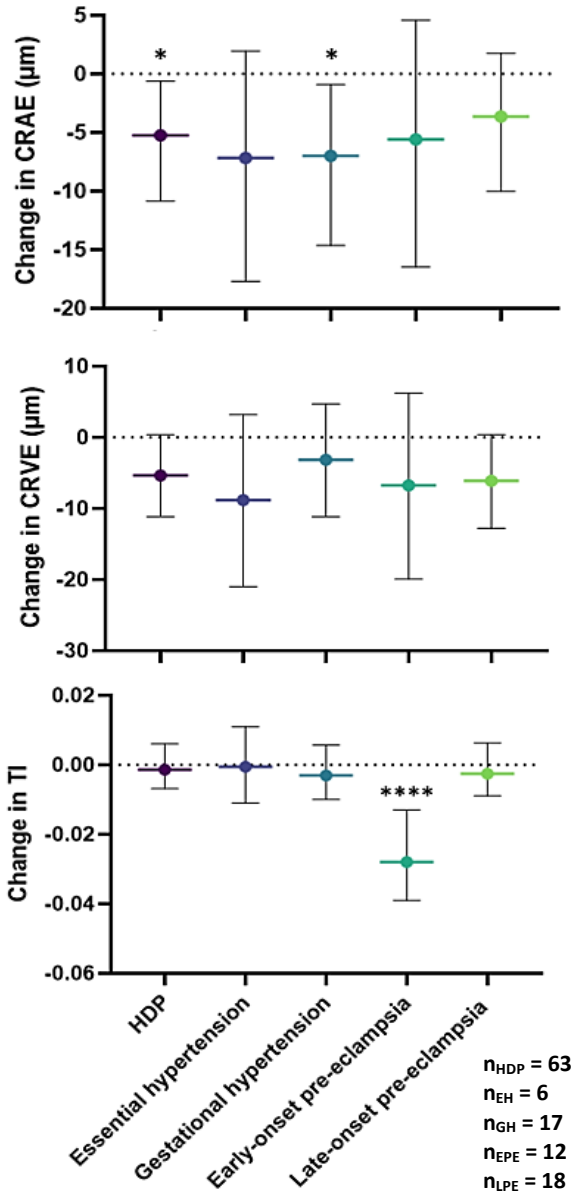

Fig. 3: Associations of exposure to HDP and the four HDP categories with CRAE, CRVE and TI in childhood, compared to non-HDP. Estimates were displayed as change (95% CI) in CRAE (µm), CRVE (µm), and TI over the total HDP group and the four HDP categories, compared to non-HDP, estimated by linear mixed effect models. The models were adjusted for child's sex, age, MAP, birthweight and BMI, mother's age, pre-pregnancy BMI and education, season of examination, batch effect of the camera resolution, and CRVE when CRAE was the dependent variable and vice versa. A negative association was found between exposure to HDP, and more specifically gestational hypertension, and the CRAE value, compared to non-HDP. Lower TI values were noted in the early-onset pre-eclampsia group compared to the non-HDP group.
CRAE = central retinal arteriolar equivalent; CRVE = central retinal venular equivalent; TI = tortuosity index; (non-)HDP = (non-) hypertensive disorders of pregnancy; EH = essential hypertension; GH = gestational hypertension; EPE = early-onset pre-eclampsia; LPE = late-onset pre-eclampsia; * = p < 0.05; **** = p < 0.0001

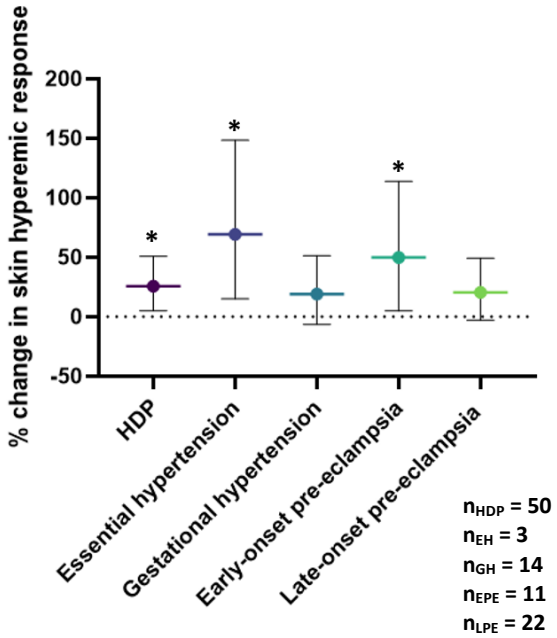

Fig. 4: Associations of exposure to HDP and the four HDP categories with the heat-induced skin hyperemic response in childhood, compared to non-HDP. Estimates were displayed as a percentage change (95% CI) in heat-induced skin hyperemic response over the total HDP group and the four HDP categories, compared to non-HDP, estimated by multiple linear regression models. These models were adjusted for child's sex, age, MAP, birthweight and BMI, mother's age, pre-pregnancy BMI and education, and season of examination, start temperature and baseline value of the measurement. A positive association was found between exposure to HDP, and more specifically essential hypertension and early-onset pre-eclampsia, and the heat-induced skin hyperemic response, compared to non-HDP.
(non-)HDP = (non-) hypertensive disorders of pregnancy; EH = essential hypertension; GH = gestational hypertension; EPE = early-onset pre-eclampsia; LPE = late-onset pre-eclampsia; * = $p < 0.05$

Adjustment for gestational age instead of birthweight did not mitigate previously reported associations between HDP exposure, and more specifically gestational hypertension, and lower CRAE values in childhood. Results for CRVE values remained unchanged after adjustment for gestational age. Associations of lower TI and specific exposure to early-onset pre-eclampsia remained after adjustment for gestational age. Additional adjustment for alcohol consumption during pregnancy in the analyses between HDP (n = 63) or the four HDP categories, and non-HDP (n = 124), did not alter the previously reported associations with CRAE, CRVE and TI. Additional adjustment for smoking during pregnancy for the analyses with HDP (n = 63) or the four HDP categories, and non-HDP (n = 125) did not influence the associations for CRAE, CRVE and TI. Adding year of follow-up examination to the analyses with HDP (n = 63) or the four HPD categories, and non-HDP (n = 126) did influence the association with CRAE. No changes in results with CRVE and TI were noticeable with addition of year of examination to the analyses.

Skin microvasculature – Gestational age (weeks) and birthweight (grams) were highly correlated ($r = 0.83$, $p < 2.2*10^{-16}$). Adjustment for gestational age instead of birthweight did not influence previously reported associations between exposure to HDP or more specifically one of the four categories of HDP, and the skin hyperemic response in childhood. Additional adjustment for alcohol consumption during pregnancy for the analysis with HDP (n = 50) or one of the four HDP categories, and non-HDP (n = 123), did not mitigate previously reported associations of higher skin hyperemic responses. Adding smoking during pregnancy for the analyses with HDP (n = 50) or one of the four HDP categories, and non-HDP (n = 124) did not influence the associations. Additional adjustment for year of follow-up examination for the analyses with HDP (n = 50) or one of the four HDP categories, and non-HDP (n = 125) did alter the associations with the skin hyperemic response.

Table 4: Results of the sensitivity analyses for (1) gestational age instead of birthweight, (2) addition of alcohol consumption during pregnancy, (3) addition of smoking during pregnancy, and (4) addition of year of follow-up examination, for the outcome variables CRAE, CRVE, TI and skin hyperemic response. Estimates (95% CI) were shown for HDP in total compared to non-HDP, and for a significant HDP category compared to non-HDP.

Outcome variable	CRAE (µm)		CRVE (µm)		TI		Skin hyperemic response (PU)	
	HDP in total and GH		*HDP in total and LPE*		*HDP in total and EPE*		*HDP in total and EH, EPE*	
(1) Gestational age	-5.37 (-11.18, -0.56)	-7.2 (-14.92, -1.04)	-6.26 (-12.33, 0.50)	-8.12 (-14.91, 0.13)	-0.001 (-0.005, 0.008)	-0.02 (-0.03, -0.002)	23.1 (2.02, 48.74)	71.6 (16.18, 153.45), 46.2 (8.52, 133.96)
(2) Alcohol consumption during pregnancy	-5.25 (-10.63, -0.68)	-6.71 (-14.16, -0.72)	-4.68 (-11.07, 0.76)	-5.36 (-12.62, 1.01)	-0.001 (-0.007, 0.006)	-0.03 (-0.04, -0.01)	26.9 (5.98, 52.2)	67 (13.87, 144.98), 53.7 (7.85, 119.46)
(3) Smoking during pregnancy	-4.98 (-10.5, -0.30)	-6.5 (-14.19, -0.36)	-5.28 (-11.75, 0.14)	-6.03 (-13.31, 0.32)	-0.001 (-0.004, 0.006)	-0.03 (-0.04, -0.01)	26.4 (5.06, 52.03)	82.4 (23, 170.47), 51.3 (5.63, 116.52)
(4) Year of follow-up examination	-4.96 (-11.13, -0.002)	-6.6 (-14.66, - 0.38)	-4.41 (-10.90, 2.09)	-4.99 (-12.45, 2.47)	-0.002 (-0.007, 0.004)	-0.03 (-0.04, -0.02)	23.4 (-16.05, 81.48)	73.3 (2.88, 191.54), 54.2 (-10.9, 166.74)

CRAE = central retinal arteriolar equivalent; CRVE = central retinal venular equivalent; TI = tortuosity index; PU = perfusion units**;** HDP = hypertensive disorders of pregnancy; GH = gestational hypertension; LPE = late-onset pre-eclampsia; EPE = early-onset pre-eclampsia; EH = essential hypertension

DISCUSSION

The aim of this study was to find associations between prenatal exposure to HDP and the morphology and functionality of the childhood microvasculature. For the microvascular morphology, a negative association was found between prenatal exposure to HDP and the retinal arteriolar diameter (µm). Particularly, gestational hypertension was associated with smaller arteriolar diameters in childhood, compared to non-HDP. In addition, exposure to the HDP category early-onset pre-eclampsia was associated with a decrease in tortuosity compared to no HDP exposure. For the microvascular functionality, a positive association was found between prenatal exposure to HDP, mainly to early-onset pre-eclampsia, and the heat-induced skin hyperemic response in childhood, compared to no HDP exposure.

The results of retinal arteriolar narrowing in offspring exposed to HDP were consistent with the findings of Yesil *et al.* (2016) within the Generation R study (38). Narrowing of the retinal arterioles is associated with higher blood pressure in school-age children (27) and higher risks of hypertension and CVD development later in life (28, 35, 36). In addition, research has indicated that 3 to 18-year-old children exposed to HDP had elevated blood pressure levels (21), and that exposure to HDP was associated with increased risk for early-onset CVD onset from birth to young adulthood (up to 40 years old) (23). Therefore, the observed altered microvascular phenotype, particularly characterized by retinal arteriolar narrowing, might form a link between HDP exposure and childhood hypertension with future CVD onset. Values of the retinal arterioles and venules were positively correlated, although the association of retinal arteriolar narrowing and HDP exposure was independent of the retinal venules. Studies have suggested that both retinal arterioles and venules may play an independent role in hypertension and CVD development; however, further investigation is required (35, 47).

The results of specific exposure to gestational hypertension and the association of narrower retinal arterioles compared to no exposure to HDP, suggest that the exposure length and maternal novelty to high blood pressure, rather than the maternal arterial and venous dysfunction in pre-eclampsia, might be crucial for the effects on the retinal microvasculature. Nonetheless, one must be careful with interpretation of these results since the sample size was relatively small (n = 17). In addition, the negative association of exposure to early-onset pre-eclampsia and the tortuosity must be cautiously interpret due to the small sample size (n = 12). Tortuosity of the retinal vessels is also associated with hypertension and CVDs (28, 48). Abnormalities in relative vascular elongation were found to be associated with these disease patterns (48). Therefore, an increased tortuosity was

expected after exposure to early-onset pre-eclampsia; however, it could be a compensation mechanism of the blood vessels to counter the influence of the exposure. No research has described effects of decreased tortuosity. This is because of the observation of more tortuous blood vessels in several disease patterns (*e.g.* transient ischemic attack, stroke and other cerebrovascular deficiencies) (49). Blood vessels are normally straight conduits that can efficiently transport blood to organs (49). Perfusion through the placenta to the fetus can be impaired during HDP, especially in early-onset pre-eclampsia, which makes suggestions that the observed decrease in tortuosity might occur to compensate for the impaired blood flow. More research into future consequences of the observed effects with larger populations is needed.

To our knowledge, this is the first study investigating the functionality of the childhood microvasculature after HDP exposure, represented by the heat-induced skin hyperemic response. The skin hyperemic response was examined in the same manner as Witters *et al.* (30). Another way to express the heat-induced hyperemic response is in percentage difference between the baseline and heated perfusion as the Maastricht Study (Sörensen *et al.*) (50). A method more suitable for higher sample sizes as the baseline value obtains more weight. Instead, this study performed an adjustment for the baseline values of the vasodilatory response in absolute values. The positive association of exposure to HDP and the vasodilatory response in children was not consistent with the hypothesis of endothelial dysfunction and increased CVD risks (51); however, it might be a compensatory response of the blood vessels to counter the influence of HDP exposure. Normally, skin perfusion over time is characterized by a stable baseline, an initial peak in blood perfusion after heating, which is predominantly mediated by local sensory nerves, and a secondary rise and a plateau phase predominantly mediated by NO (37, 52). Experimental animal model studies found that basal and acetylcholine-induced NO production was decreased in a simulating HDP reduced-uterine-artery-perfusion rat model. In addition, these studies have indicated that there may be a compensatory up-regulation of NO-independent pathways to maintain the vasodilatory response (53). Due to the possible impaired perfusion to the fetus during HDP, especially in early-onset pre-eclampsia, suggestions are made that an increased vasodilatory response might occur with NO-independent pathway upregulations, to compensate for the adverse effects on the vessel functionality. Future consequences of these observations must be examined. Since the sample size of the essential hypertension category was only 3, the observed association was negligible and must be further analyzed within a larger sample. Interpretation of the positive association of specific exposure to early-onset pre-eclampsia and the vasodilatory response must also be made carefully due to the small sample size (n = 11); however, it might suggest that maternal arterial and venous dysfunction, with possible impaired blood flow to the fetus, is important in the compensatory response of the microvascular functionality. Further investigation with larger populations is required.

Within this study, no correlation or association was found between the retinal microvascular parameters and the skin hyperemic response within the HDP group, which could indicate intertwined mechanisms of the observed effects.

The exact mechanisms behind the associations of HDP exposure and the adverse cardiovascular effects in the offspring are unknown. Hypertension during pregnancy is a consequence of cardiovascular maladaptations occurring in the first trimester of pregnancy with provocation of increased vascular resistance (7, 9, 54). The maternal hemodynamics differ in each pregnancy trimester from the normal cardiovascular system and aberrations become more prominent when disease onset approaches (9, 11). Literature describes several hypotheses based on animal models and epidemiological findings; however, it is difficult to unravel the exact mechanisms since an ideal animal model does not exist yet, due to the unique humane condition of HDP (53). One suggests that direct effects of abnormal placental vascularization with defective trophoblastic invasion and maternal endothelial dysfunction (1, 2, 9, 13) is involved, which are likely to subsequently cause hypoxia and reduced uterine perfusion to the fetus (53). Furthermore, inflammation and oxidative stress is hypothesized to cause effects (2, 53), and genetic, epigenetic and altered microRNA expression, such as the renin-angiotensin-aldosterone mRNA upregulation might also be involved (1, 3, 22, 53). All these mechanisms could contribute to vascular remodeling and adapted

vascular functionality in the fetus. This is because the microvascular vessels undergo extensive maturation during fetal development, making them sensitive to intrauterine changes (31). These adaptations might subsequently lead to (childhood) hypertension and future CVD onset (26, 34, 53). Although, long-term monitoring after exposure to HDP is required to gather more insights into the adverse or even protective consequences of the observed microvascular effects.

Remarkable was that both the associations of the retinal and skin microvasculature were independent of prematurity variables: *i.e.* birthweight (grams) and gestational age (weeks). These parameters could be regulating factors since several studies indicated associations of birthweight and gestational age with the microvasculature (55, 56). Results of associations became stronger when prematurity was not considered, which suggests that it might be involved, but does not entirely clarifies the effect. Moreover, the associations were not influenced by and thus independent of the child's MAP, a parameter of the general cardiovascular health. Sensitivity analysis showed that the associations were also independent of maternal alcohol consumption and smoking during pregnancy. Associations for both the retinal (CRAE) and skin microvasculature were influenced by the year of follow-up examination. A possible impact of the significant difference in camera resolutions throughout the years of examination ($p < 2*10^{-16}$), must be considered in the analyses with CRAE. For the skin microvasculature, there is a possible effect of the significant difference in season of follow-up examination throughout the years ($p = 3.7*10^{-9}$), and the start temperature of the measurement was correlated with year of follow-up examination ($r = -0.3$, $p = 2.2*10^{-5}$). Adjustment for year of follow-up examination may lead to overcorrection and alteration of previously observed associations.

A case-control design with a 1:2 ratio was opted for the retinal microvascular analyses due to the relative large non-HDP group, and to gather more similar groups, increasing statistical power. By selecting more than one control per case, statistical confidence can be improved (57). The optimal pair matching method was more accurate for this study population than the "greedy" nearest neighbor matching method, because optimal matching takes the overall set of matches into account when choosing individual matches, minimizing the global distance measure (58). Therefore, more well-matched pairs were made, which is preferred for case and control groups with significantly different ages. On the contrary, a case-cohort design with constrained full matching was chosen for the skin microvasculature because of the relative small non-HDP group and to avoid selection bias. Constrained full matching with two or three controls per case increased precision of the analyses compared to normal full matching, by reducing non-homogeneity (59). Based on the effective sample size (ESS), the constrained full match ratio of 1:2 or 1:3 was chosen. A larger ESS will yield a more precise estimate of the exposure effect with weighted regression (60, 61).

This study has several strengths and limitations. A strength is that both microvascular morphology and functionality were considered within the populations to gather more insights. This is, to the best of our knowledge, the first study investigating the childhood microvascular functionality based on the heat-induced skin hyperemic response after HDP exposure. Another strength is that the four HDP categories were compared with non-HDP to create more specific hypotheses for mechanistic research. The most important limitation of this study is the small sample size of the HDP population, mainly in the four HDP categories. Therefore, interpretation of the results must be taken carefully. A second major limitation is the fact that several possible confounding factors were not considered. For example, air pollution exposure or ethnicity were not examined in the analyses, due to missing data. Luyten *et al.* found associations of prenatal and postnatal ambient air pollution with childhood retinal vessel alterations, and Witters *et al.* found that prenatal exposure to black carbon and particulate air pollution was associated with childhood skin hyperemia (29, 30). In addition, ethnicity can cover lifestyle related factors such as nutritional patterns, which might have an effect (62); however, ethnicity is also related to pre-pregnancy BMI and socio-economic status of the mother. Furthermore, genetic or epigenetic factors were not involved in the analyses, while these could have an impact on the observed effects (2, 22, 28, 62). Furthermore, stress can possibly influence laser Doppler measurements (37). However, an attempt was made to reassure the child by the

presence of the mother and watching a video during the full measurement. Another limitation is that the MAP data for the non-HDP group were not taken at the same moment as the skin perfusion measurements, which were performed during house visits. Although, MAP normally stays relatively stable due to regulating mechanisms ensuring sufficient blood flow to organs (63).

CONCLUSION

Prenatal exposure to HDP was both associated with narrowing of the retinal arterioles and an increased heat-induced skin hyperemic response. Moreover, exposure to gestational hypertension in particular was associated with narrower retinal arterioles, and specific exposure to early-onset pre-eclampsia was associated with decreased tortuosity and an increased vasodilatory response. Due to the small sample sizes within the four HDP categories, interpretations must be made carefully. However, the findings suggest that an altered microvascular phenotype might form a link between HDP exposure and childhood hypertension with future cardiovascular disease onset. In addition, the increased vasodilatory function might be a compensatory response of the blood vessels after exposure to HDP. More investigation into the future consequences of the observed effects and the related mechanisms, within larger populations, is required.

REFERENCES

1. Fox R, Kitt J, Leeson P, Aye CYL, Lewandowski AJ. Preeclampsia: Risk Factors, Diagnosis, Management, and the Cardiovascular Impact on the Offspring. J Clin Med. 2019;8(10).
2. Pinheiro TV, Brunetto S, Ramos JG, Bernardi JR, Goldani MZ. Hypertensive disorders during pregnancy and health outcomes in the offspring: a systematic review. J Dev Orig Health Dis. 2016;7(4):391-407.
3. Park K, Wei J, Minissian M, Bairey Merz CN, Pepine CJ. Adverse Pregnancy Conditions, Infertility, and Future Cardiovascular Risk: Implications for Mother and Child. Cardiovasc Drugs Ther. 2015;29(4):391-401.
4. Fox H, Callander EJ. The cost of Hypertensive Disorders of Pregnancy to the Australian healthcare system. Pregnancy Hypertens. 2020;21:197-9.
5. Umesawa M, Kobashi G. Epidemiology of hypertensive disorders in pregnancy: prevalence, risk factors, predictors and prognosis. Hypertens Res. 2017;40(3):213-20.
6. Bruce A. White SPP. Endocrine and reproductive physiology Fourth edition ed. Philadelphia Elsevier Mosby 2013.
7. Gyselaers W. Maternal Venous Hemodynamic Dysfunction in Proteinuric Gestational Hypertension: Evidence and Implications. J Clin Med. 2019;8(3).
8. Ying W, Catov JM, Ouyang P. Hypertensive Disorders of Pregnancy and Future Maternal Cardiovascular Risk. J Am Heart Assoc. 2018;7(17):e009382.
9. Vonck S. Doctoral Dissertation - Maternal cardiovascular function: Closing the circle. Hasselt University: Flanders State of the Art 2018. 181 p.
10. Steegers EA, von Dadelszen P, Duvekot JJ, Pijnenborg R. Pre-eclampsia. Lancet. 2010;376(9741):631-44.
11. Gyselaers W, Thilaganathan B. Preeclampsia: a gestational cardiorenal syndrome. J Physiol. 2019;597(18):4695-714.
12. Staff AC. The two-stage placental model of preeclampsia: An update. J Reprod Immunol. 2019;134-135:1-10.
13. Dimuthu Vinayagam KL, Asma Khalil, Baskaran Thilaganathan. Preeclampsia - What is to blame? The placenta, maternal cardiovascular system or both? World Journal of Obstetrics and Gynecology 2015.

14. Garovic VD, White WM, Vaughan L, Saiki M, Parashuram S, Garcia-Valencia O, et al. Incidence and Long-Term Outcomes of Hypertensive Disorders of Pregnancy. J Am Coll Cardiol. 2020;75(18):2323-34.
15. Benschop L, Schalekamp-Timmermans S, Roeters van Lennep JE, Jaddoe VWV, Wong TY, Cheung CY, et al. Gestational hypertensive disorders and retinal microvasculature: the Generation R Study. BMC Med. 2017;15(1):153.
16. Weissgerber TL, Turner ST, Bailey KR, Mosley TH, Jr., Kardia SL, Wiste HJ, et al. Hypertension in pregnancy is a risk factor for peripheral arterial disease decades after pregnancy. Atherosclerosis. 2013;229(1):212-6.
17. Wadhwa PD, Buss C, Entringer S, Swanson JM. Developmental origins of health and disease: brief history of the approach and current focus on epigenetic mechanisms. Semin Reprod Med. 2009;27(5):358-68.
18. de Boo HA, Harding JE. The developmental origins of adult disease (Barker) hypothesis. Aust N Z J Obstet Gynaecol. 2006;46(1):4-14.
19. Perak AM, Lancki N, Kuang A, Labarthe DR, Allen NB, Shah SH, et al. Associations of Maternal Cardiovascular Health in Pregnancy With Offspring Cardiovascular Health in Early Adolescence. JAMA. 2021;325(7):658-68.
20. Miliku K, Bergen NE, Bakker H, Hofman A, Steegers EA, Gaillard R, et al. Associations of Maternal and Paternal Blood Pressure Patterns and Hypertensive Disorders during Pregnancy with Childhood Blood Pressure. J Am Heart Assoc. 2016;5(10).
21. Jansen MA, Pluymen LP, Dalmeijer GW, Groenhof TKJ, Uiterwaal CS, Smit HA, et al. Hypertensive disorders of pregnancy and cardiometabolic outcomes in childhood: A systematic review. Eur J Prev Cardiol. 2019;26(16):1718-47.
22. Hammad IA, Meeks H, Fraser A, Theilen LH, Esplin MS, Smith KR, et al. Risks of cause-specific mortality in offspring of pregnancies complicated by hypertensive disease of pregnancy. Am J Obstet Gynecol. 2020;222(1):75 e1- e9.
23. Huang C, Li J, Qin G, Liew Z, Hu J, Laszlo KD, et al. Maternal hypertensive disorder of pregnancy and offspring early-onset cardiovascular disease in childhood, adolescence, and young adulthood: A national population-based cohort study. PLoS Med. 2021;18(9):e1003805.
24. Lowe Sa. STEVENS & LOWE'S HUMAN HISTOLOGY, FOURTH EDITION. Philadelphia, PA 19103-2899: Elsevier, Mosby; 2015.
25. Boulpaep WBaE. Medical Physiology, Third edition. Philadelphia: Elsevier; 2017.
26. Guven G, Hilty MP, Ince C. Microcirculation: Physiology, Pathophysiology, and Clinical Application. Blood Purif. 2020;49(1-2):143-50.
27. Gishti O, Jaddoe VW, Felix JF, Klaver CC, Hofman A, Wong TY, et al. Retinal microvasculature and cardiovascular health in childhood. Pediatrics. 2015;135(4):678-85.
28. Cheung CY, Ikram MK, Sabanayagam C, Wong TY. Retinal microvasculature as a model to study the manifestations of hypertension. Hypertension. 2012;60(5):1094-103.
29. Luyten LJ, Dockx Y, Provost EB, Madhloum N, Sleurs H, Neven KY, et al. Children's microvascular traits and ambient air pollution exposure during pregnancy and early childhood: prospective evidence to elucidate the developmental origin of particle-induced disease. BMC Med. 2020;18(1):128.
30. Witters K, Dockx Y, Op't Roodt J, Lefebvre W, Vanpoucke C, Plusquin M, et al. Dynamics of skin microvascular blood flow in 4-6-year-old children in association with pre- and postnatal black carbon and particulate air pollution exposure. Environ Int. 2021;157:106799.
31. Clough GF, Norman M. The microcirculation: a target for developmental priming. Microcirculation. 2011;18(4):286-97.
32. Struijker-Boudier HA, Heijnen BF, Liu YP, Staessen JA. Phenotyping the microcirculation. Hypertension. 2012;60(2):523-7.
33. Erik H. Serné RTdJ, Etto C. Eringa, Richard G. IJzerman and Coen D.A. Stehouwer. Microvascular Dysfunction. Hypertension. 2007.

34. Feihl F, Liaudet L, Levy BI, Waeber B. Hypertension and microvascular remodelling. Cardiovasc Res. 2008;78(2):274-85.
35. Ding J, Wai KL, McGeechan K, Ikram MK, Kawasaki R, Xie J, et al. Retinal vascular caliber and the development of hypertension: a meta-analysis of individual participant data. J Hypertens. 2014;32(2):207-15.
36. Seidelmann SB, Claggett B, Bravo PE, Gupta A, Farhad H, Klein BE, et al. Retinal Vessel Calibers in Predicting Long-Term Cardiovascular Outcomes: The Atherosclerosis Risk in Communities Study. Circulation. 2016;134(18):1328-38.
37. Roustit M, Cracowski JL. Non-invasive assessment of skin microvascular function in humans: an insight into methods. Microcirculation. 2012;19(1):47-64.
38. Yesil GD, Gishti O, Felix JF, Reiss I, Ikram MK, Steegers EA, et al. Influence of Maternal Gestational Hypertensive Disorders on Microvasculature in School-Age Children: The Generation R Study. Am J Epidemiol. 2016;184(9):605-15.
39. Janssen BG, Madhloum N, Gyselaers W, Bijnens E, Clemente DB, Cox B, et al. Cohort Profile: The ENVIRonmental influence ON early AGEing (ENVIRONAGE): a birth cohort study. Int J Epidemiol. 2017;46(5):1386-7m.
40. University H. Limburgs Pre-eclampsie Onderzoek - LimPrOn: Hasselt University 2022 [Available from: https://www.uhasselt.be/zwangerschapsvergiftiging#anch-5d9-limburgs-pre-eclampsie-onderzoek-limpron.
41. World Medical A. World Medical Association Declaration of Helsinki: ethical principles for medical research involving human subjects. JAMA. 2013;310(20):2191-4.
42. Canon. Manual: CR-2 PLUS AF Digital Non-Mydriatic Retinal Camera: Canon USA; 2013 [Available from: https://www.usa.canon.com/internet/portal/us/home/support/details/eyecare/digital-non-mydriatic-retinal-cameras/cr-2-plus-af?tab=manuals.
43. Perimed. SKIN PROBES - PROBE 457 Thermostatic Small-Angled Probe: Perimed AB; 2020 [Available from: https://www.perimed-instruments.com/content/laser-doppler-probes-perimed/.
44. Le Brocq M, Leslie SJ, Milliken P, Megson IL. Endothelial dysfunction: from molecular mechanisms to measurement, clinical implications, and therapeutic opportunities. Antioxid Redox Signal. 2008;10(9):1631-74.
45. Braverman IM, Schechner JS, Silverman DG, Keh-Yen A. Topographic mapping of the cutaneous microcirculation using two outputs of laser-Doppler flowmetry: flux and the concentration of moving blood cells. Microvasc Res. 1992;44(1):33-48.
46. Parati G, Stergiou GS, Asmar R, Bilo G, de Leeuw P, Imai Y, et al. European Society of Hypertension guidelines for blood pressure monitoring at home: a summary report of the Second International Consensus Conference on Home Blood Pressure Monitoring. J Hypertens. 2008;26(8):1505-26.
47. Ikram MK, de Jong FJ, Vingerling JR, Witteman JC, Hofman A, Breteler MM, et al. Are retinal arteriolar or venular diameters associated with markers for cardiovascular disorders? The Rotterdam Study. Invest Ophthalmol Vis Sci. 2004;45(7):2129-34.
48. Ciurica S, Lopez-Sublet M, Loeys BL, Radhouani I, Natarajan N, Vikkula M, et al. Arterial Tortuosity. Hypertension. 2019;73(5):951-60.
49. Han HC. Twisted blood vessels: symptoms, etiology and biomechanical mechanisms. J Vasc Res. 2012;49(3):185-97.
50. Sorensen BM, Houben AJ, Berendschot TT, Schouten JS, Kroon AA, van der Kallen CJ, et al. Prediabetes and Type 2 Diabetes Are Associated With Generalized Microvascular Dysfunction: The Maastricht Study. Circulation. 2016;134(18):1339-52.
51. Touwslager RN, Houben AJ, Gielen M, Zeegers MP, Stehouwer CD, Zimmermann LJ, et al. Endothelial vasodilatation in newborns is related to body size and maternal hypertension. J Hypertens. 2012;30(1):124-31.
52. Minson CT. Thermal provocation to evaluate microvascular reactivity in human skin. J Appl Physiol (1985). 2010;109(4):1239-46.

53. Davis EF, Newton L, Lewandowski AJ, Lazdam M, Kelly BA, Kyriakou T, et al. Pre-eclampsia and offspring cardiovascular health: mechanistic insights from experimental studies. Clin Sci (Lond). 2012;123(2):53-72.
54. Foo FL, Mahendru AA, Masini G, Fraser A, Cacciatore S, MacIntyre DA, et al. Association Between Prepregnancy Cardiovascular Function and Subsequent Preeclampsia or Fetal Growth Restriction. Hypertension. 2018;72(2):442-50.
55. Gishti O, Jaddoe VW, Duijts L, Steegers E, Reiss I, Hofman A, et al. Impact of birth parameters and early life growth patterns on retinal microvascular structure in children: The Generation R Study. J Hypertens. 2015;33(7):1429-37.
56. Parizotto GP, de Souza LV, Thomazini F, Prado MS, Agudelo JSH, de Almeida DC, et al. Birth weight and its relationship with endothelial function and pattern of endothelium-derived microparticles during childhood: New insight about early vascular damage. Life Sci. 2022;298:120517.
57. Journal BM. Chapter 8. Case-control and cross sectional studies 2021 [Available from: https://www.bmj.com/about-bmj/resources-readers/publications/epidemiology-uninitiated/8-case-control-and-cross-sectional.
58. Stuart EA. Matching methods for causal inference: A review and a look forward. Stat Sci. 2010;25(1):1-21.
59. Elizabeth A Stuart KMG. Using full matching to estimate causal effects in nonexperimental studies: examining the relationship between adolescent marijuana use and adult outcomes. Developmental psychology. 2008.
60. Greifer N. Appendix 1: Using cobalt with Other Preprocessing Packages: CRAN.R; 2022 [Available from: https://cran.r-project.org/web/packages/cobalt/vignettes/cobalt_A1_other_packages.html.
61. Pustejovsky JE. Effective sample size aggregation: jepusto.com; 2019 [Available from: https://www.jepusto.com/effective-sample-size-aggregation/.
62. Houben A, Martens RJH, Stehouwer CDA. Assessing Microvascular Function in Humans from a Chronic Disease Perspective. J Am Soc Nephrol. 2017;28(12):3461-72.
63. DeMers D, Wachs D. Physiology, Mean Arterial Pressure. StatPearls. Treasure Island (FL)2022.

Acknowledgements – The authors thank the follow-up examination team for performing the measurements on mother-child pairs throughout the years. The authors acknowledge Leen Rasking for analyses of the retinal photographs. Michelle Plusquin and Hanne Sleurs are acknowledged for assistance with data analyses. Janne Pauwels gratefully acknowledges Hanne Sleurs for providing feedback on the report.

Author contributions – M.P. and H.S. designed the research. H.S., J.P. and the rest of the follow-up examination team performed the measurements on mother-child pairs. J.P. executed data analysis. J.P. wrote the report and H.S. carefully edited the manuscript.

SUPPORTING INFORMATION

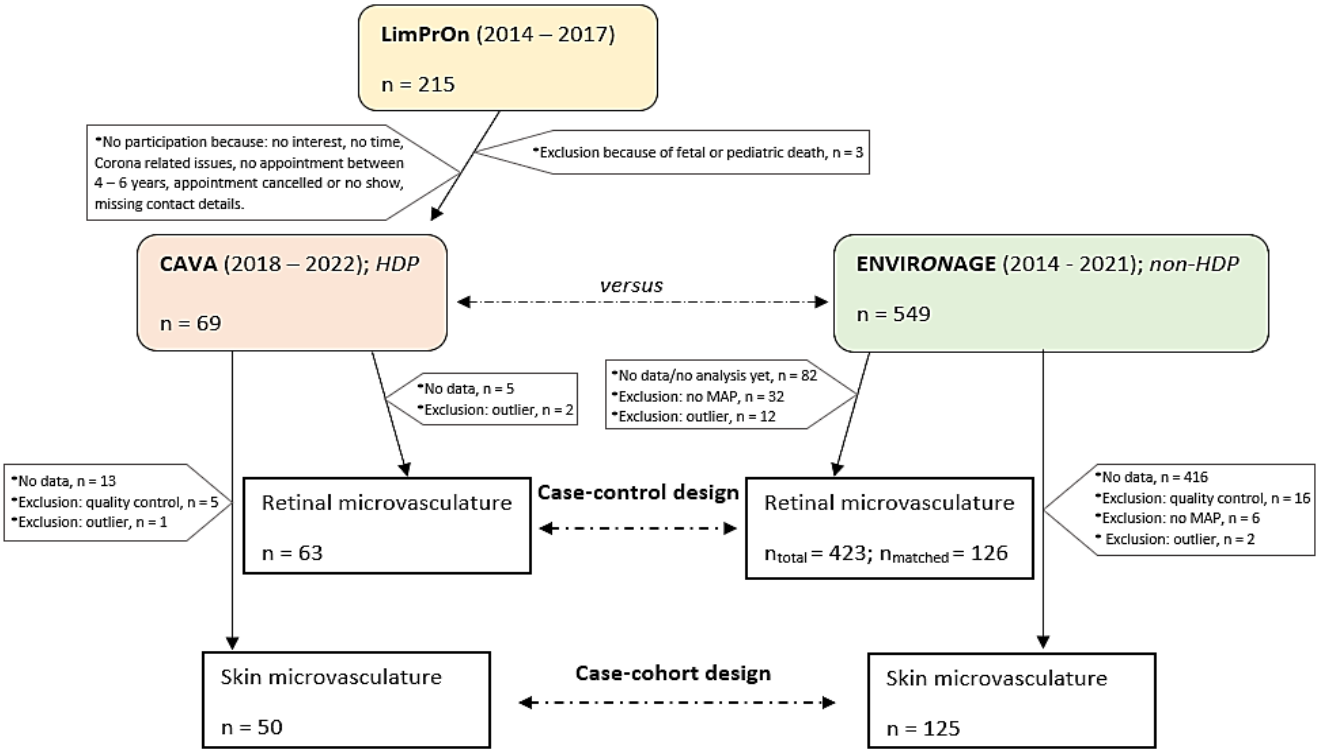

Fig. S1: Flowchart of the selection procedure. The participants of the HDP group (n = 69) were recruited from the LimPrOn study (n = 215), four to six years after birth in 2014 – 2017. The results of retinal and skin microvasculature of HDP were compared with that of the non-HDP group in a case-control and case-cohort design, respectively. Exclusion of data was applied after quality control and statistical outlier detection (threshold 3 times the standard deviation (SD) of the mean). In addition, participants with no mean arterial pressure data (MAP) were excluded.

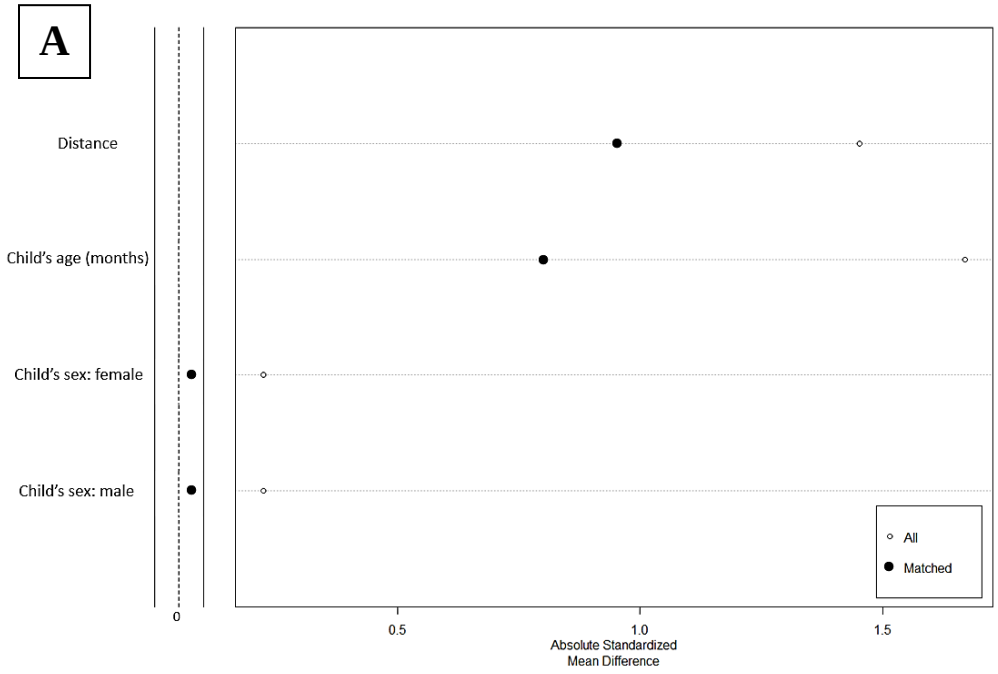

B

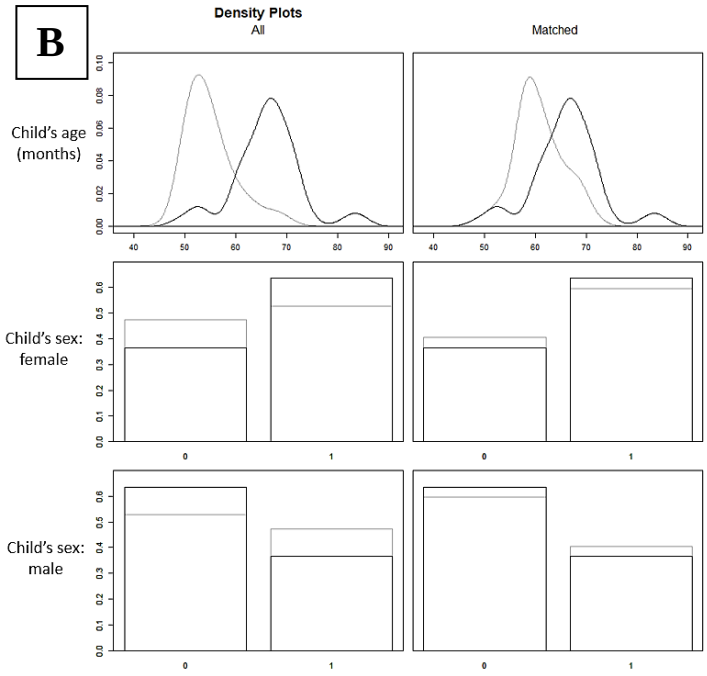

C

	SMDs	Var. ratios	eCDF mean & maximum
Unmatched data: N = 63 HDP *versus* 423 non-HDP			
Distance	1.45	3.61	0.40 | 0.75
Child's age (months)	1.67	1.81	0.41 | 0.76
Child's sex: female	0.22	.	0.11 | 0.11
Child's sex: male	-0.22	.	0.11 | 0.11
Matched data: N = 63 HDP *versus* 126 non-HDP			
Distance	0.95	1.75	0.12 | 0.50
Child's age (months)	0.80	1.98	0.13 | 0.48
Child's sex: female	0.08	.	0.04 | 0.04
Child's sex: male	-0.08	.	0.04 | 0.04

Fig. S2: Balance assessment of the matching methods: Optimal pair 1:2 matching. (A) The Love plot showed balance of the standardized mean differences (SMDs), which are the differences in the means of each covariate between the HDP and non-HDP group standardized to the same scale for all covariates. SMDs close to zero indicate good balance. Optimal pair 1:2 matching showed improved balance for the covariates child's age (months) and child's sex. **(B)** The density plot displayed the values of the covariates on the x-axis and the density of the population at that covariate value on the y-axis. For child's sex (binary variable), the y-axis displayed the proportion of the population at that covariate value. The black line corresponds to the HDP group and the gray line to the non-HDP group. Optimal pair 1:2 matching improved the balance of the covariates child's age (months) and child's sex between the HDP and non-HDP group. **(C)** The table showed the values of the SMDs, the variance ratios (var. ratios) and the empirical CDF statistics (eCDF mean and maximum). Variance ratios show the ratio of the variance of a covariate in the HDP group to that in the non-HDP group. These ratios should be close to one, so that the variance of the populations are similar. Recommendation for variance ratios is to be between 0.5 and 2. Empirical CDF statistics correspond to the difference in the overall distribution of the covariates between the HDP and non-HDP group. Values for eCDF mean and maximum closer to zero indicate better balance. Matching of the HDP group with the non-HDP based on child's age (months) and sex improved balance between the two groups.

A

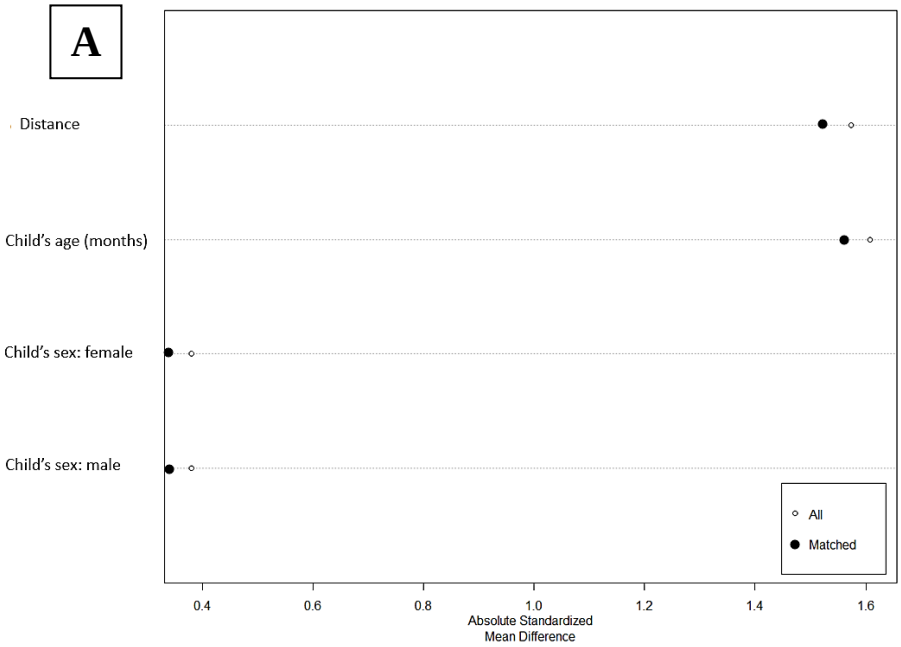

B

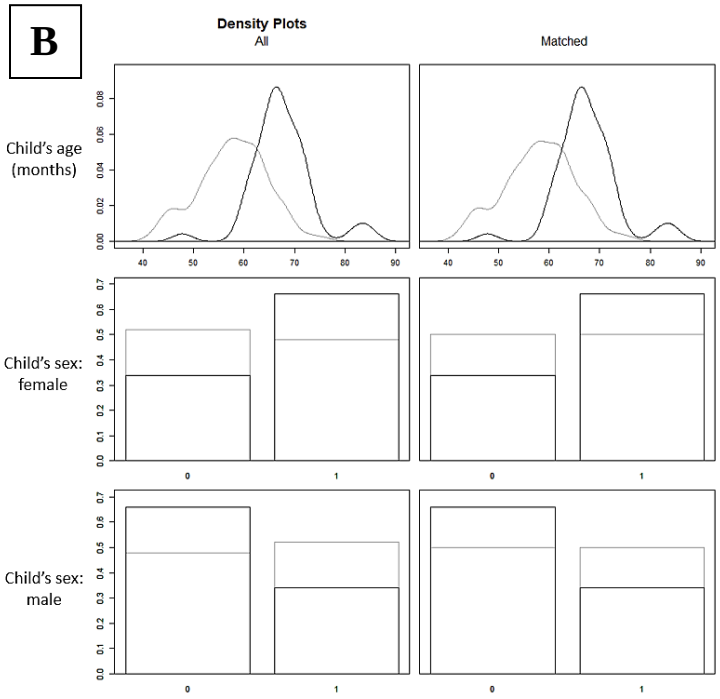

C

	SMDs	Var. ratios	eCDF mean & maximum
Unmatched data: N = 50 HDP *versus* 125 non-HDP			
Distance	1.57	1.58	0.38 | 0.65
Child's age (months)	1.61	0.79	0.36 | 0.64
Child's sex: female	0.38	.	0.18 | 0.18
Child's sex: male	-0.38	.	0.18 | 0.18
Matched data: N = 50 HDP *versus* 125 non-HDP			
Distance	1.52	1.4037	0.37 | 0.62
Child's age (months)	1.56	0.7569	0.35 | 0.62
Child's sex: female	0.34	.	0.16 | 0.16
Child's sex: male	-0.34	.	0.16 | 0.16
ESS: N = 120			

Fig. S3: Balance assessment of the matching methods: Constrained full matching with a 1:2 / 1:3 ratio. Normal full matching lead to non-homogeneous ratios of HDP *versus* non-HDP, with most extreme comparisons of seven HDP samples matched to one non-HDP sample and one HDP sample matched to 49 non-HDP samples. Constrained full matching made these comparisons more homogeneous to minimize variance in the resulting effect estimates. A minimum of two and a maximum of three non-HDP matches with one HDP sample was created based on the highest "effective sample size (ESS)". The ESS shows the effective sample size resulting from the matching weights. Constrained full matching gathered an ESS of 120, while normal full matching gathered an ESS of only 14.51. **(A)** The Love plot showed balance of the standardized mean differences (SMDs), which are the differences in the means of each covariate between the HDP and non-HDP group standardized to the same scale for all covariates. SMDs close to zero indicate good balance. Constrained full matching showed slightly improved balance for the covariates child's age (months) and child's sex. **(B)** The density plot displayed the values of the covariates on the x-axis and the density of the population at that covariate value on the y-axis. For child's sex (binary variable), the y-axis displayed the proportion of the population at that covariate value. The black line corresponds to the HDP group and the gray line to the non-HDP group. Constrained full matching slightly improved the balance of the covariates child's age (months) and child's sex between the HDP and non-HDP group. **(C)** The table showed the values of the SMDs, the variance ratios (var. ratios) and the empirical CDF statistics (eCDF mean and maximum). Variance ratios show the ratio of the variance of a covariate in the HDP group to that in the non-HDP group. These ratios should be close to one, so that the variance of the populations are similar. Recommendation for variance ratios is to be between 0.5 and 2. Empirical CDF statistics correspond to the difference in the overall distribution of the covariates between the HDP and non-HDP group. Values for eCDF mean and maximum closer to zero indicate better balance. Matching of the HDP group with the non-HDP based on child's age (months) and sex improved balance between the two groups.

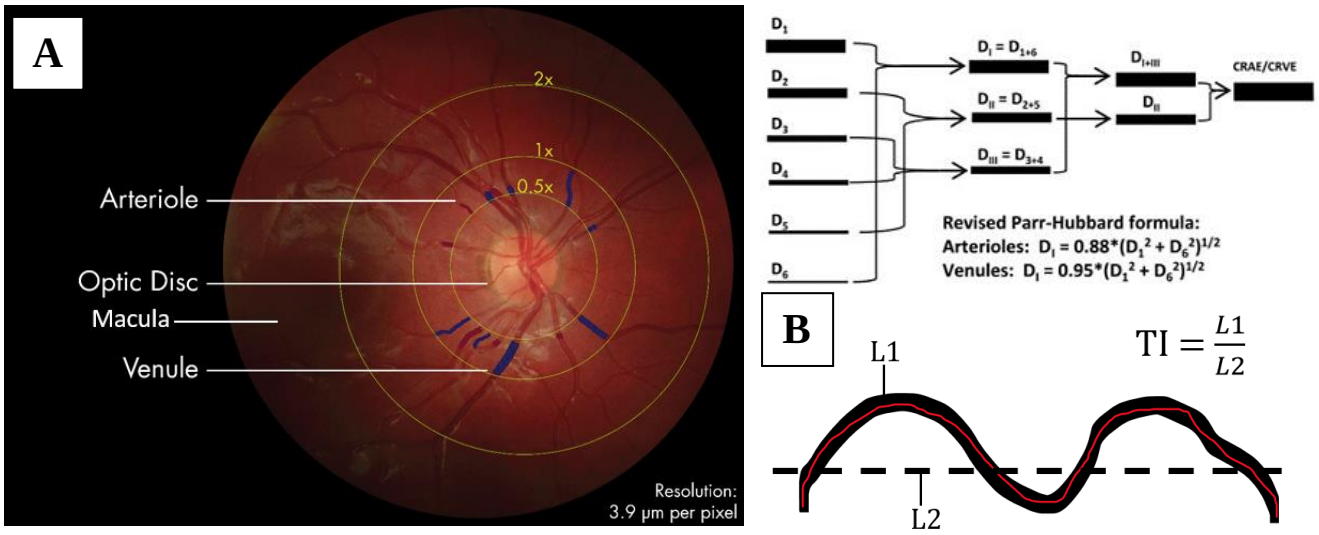

Fig. S4: Picture of the retinal photograph and analysis in the MONA-REVA software. (A) The central retinal arteriolar equivalent (CRAE) and central retinal venular equivalent (CRVE) were calculated with the revised Parr-Hubbard formula, by determining the six largest arterioles and six largest venules within 0.5 and 1 times the diameter of the optic disc (OD), starting from its margin. Arterioles within this area are indicated in red, the venules in blue. The macula or "yellow spot" represents the black circle at the left side of the picture. This picture was taken from the right eye. (29) **(B)** The tortuosity index (TI), as measure of the curvature of the vessels, was calculated between 1.5 and 5 times the radius of the OD and represents the ratio between the length along the centerline (L1) and the linear distance between the two end points (L2).

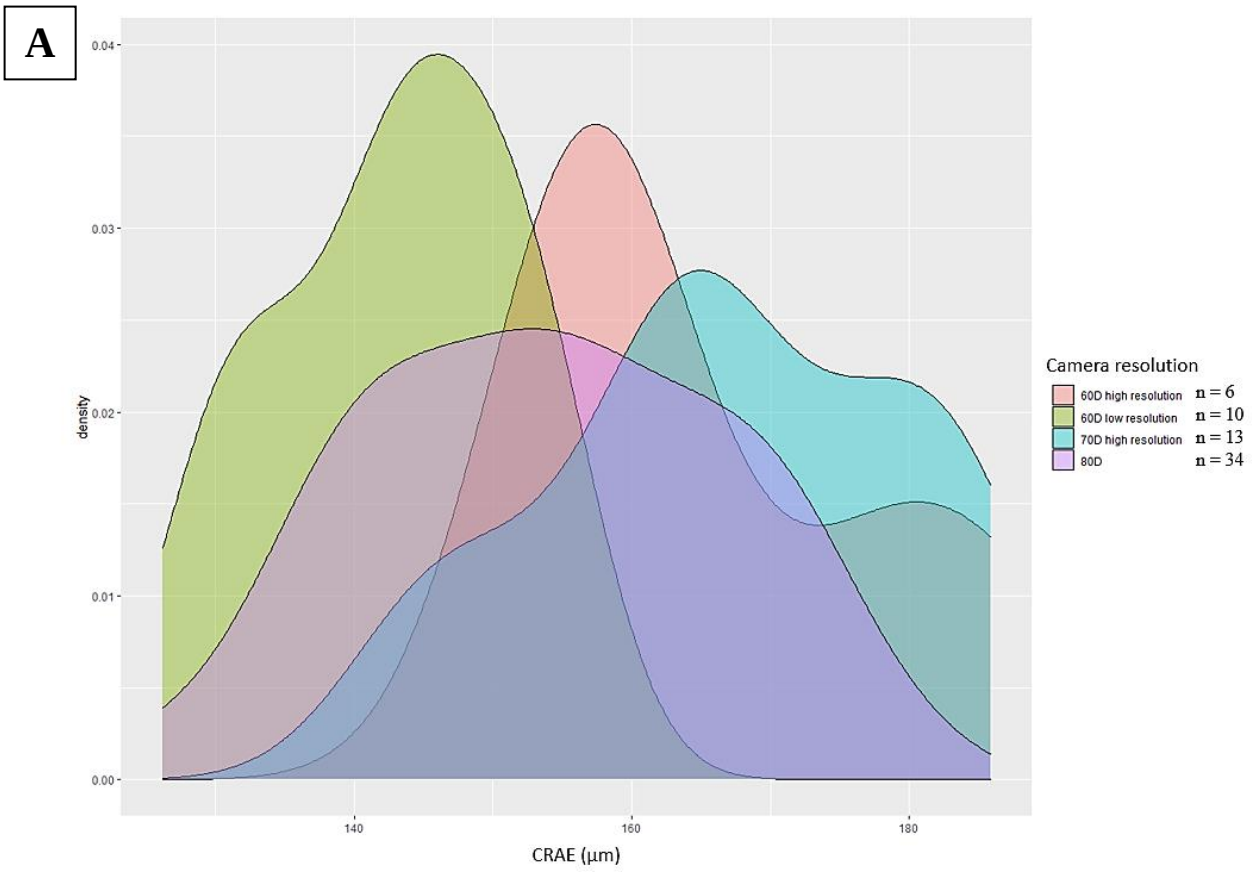

B

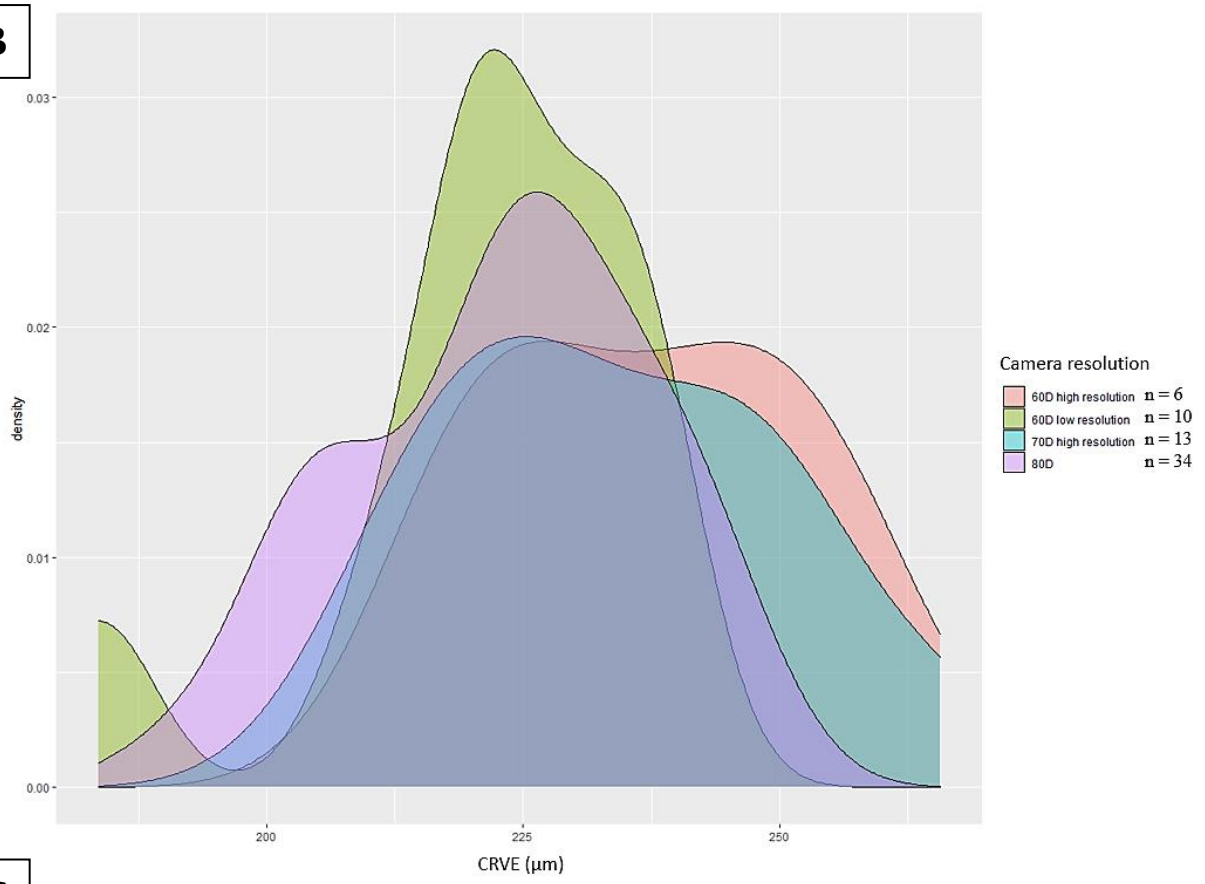
0.03
0.02
0.01
0.00
density
200
225
250
CRVE (µm)
Camera resolution
60D high resolution n = 6
60D low resolution n = 10
70D high resolution n = 13
80D n = 34

C

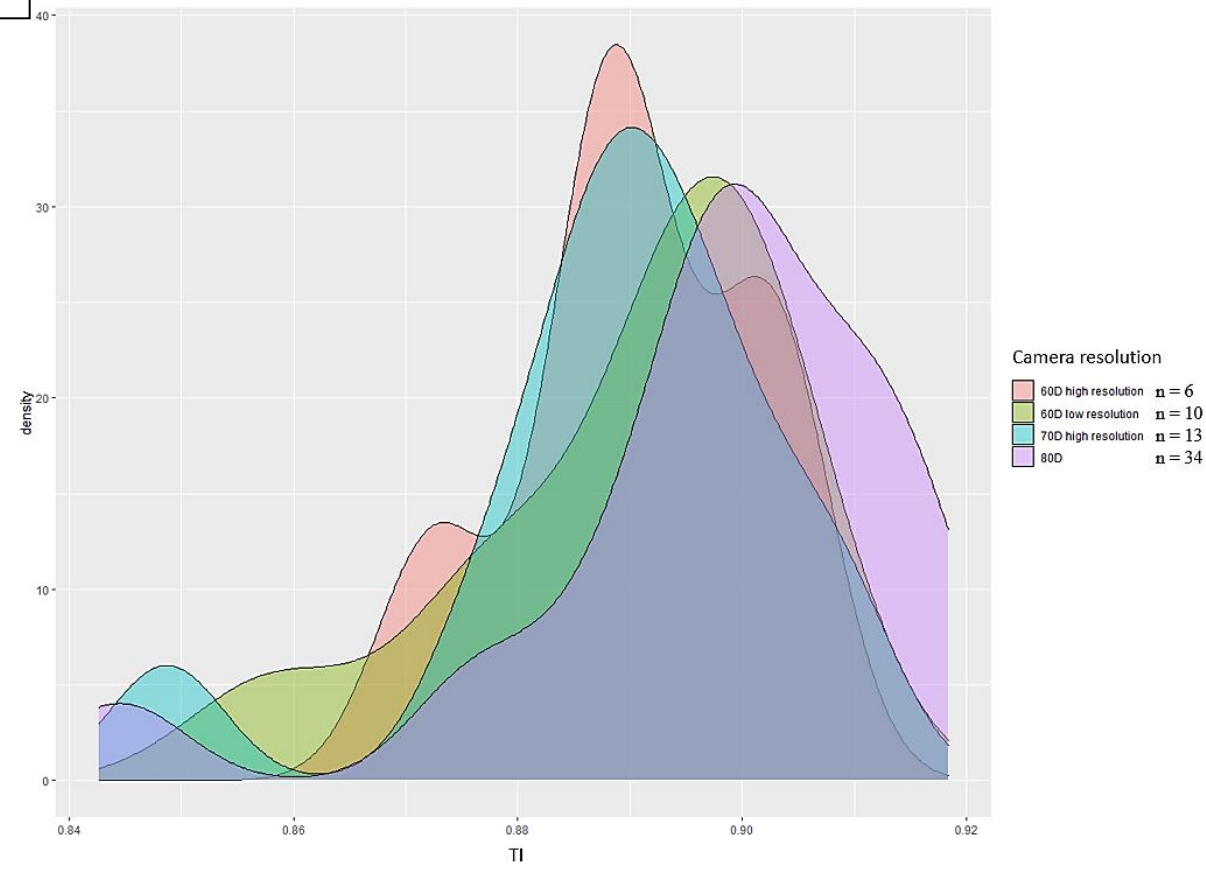
40
30
20
10
0
density
0.84
0.86
0.88
0.90
0.92
TI
Camera resolution
60D high resolution n = 6
60D low resolution n = 10
70D high resolution n = 13
80D n = 34

Fig. S5: Assessing the batch effect of the different camera resolutions. Density overlap plots of the outcome variables CRAE (µm) (A), CRVE (µm) (B) and TI (C) in the HDP group. On the x-axis, the values of the CRAE (µm) (A), CRVE (µm) (B) and TI (C) were displayed, on the y-axis the density of the values within the HDP population. The plots were colored based on camera resolution: red for 60D high resolution (n = 6), green for 60D low resolution (n = 10), blue for 70D high resolution (n = 13) and purple for 80D resolution (n = 34). The most remarkable effect was observed for the CRAE values: the 60D low resolution camera gave visually lower CRAE values, while the 70D high resolution gave visually higher CRAE values. One-way ANOVA tests showed that the values of CRAE and CRVE were significantly different throughout the different camera resolutions for both the HDP group (CRAE: $p = 9*10^{-5}$; CRVE: p = 0.04) and non-HDP group (CRAE: p = 0.05; CRVE: p = 0.04). The 60D low resolutions showed lower CRAE values compared to the 60D and 70D high resolution (p = 0.005; p = 0.0001), and the 80D resolution obtained lower CRAE values compared to the 70D high resolution (p = 0.01) (Tukey's HSD post hoc test). The values of the TI appeared not to be influenced by the different camera resolutions in both the HDP group (p = 0.35) and non-HDP group (p = 0.09).

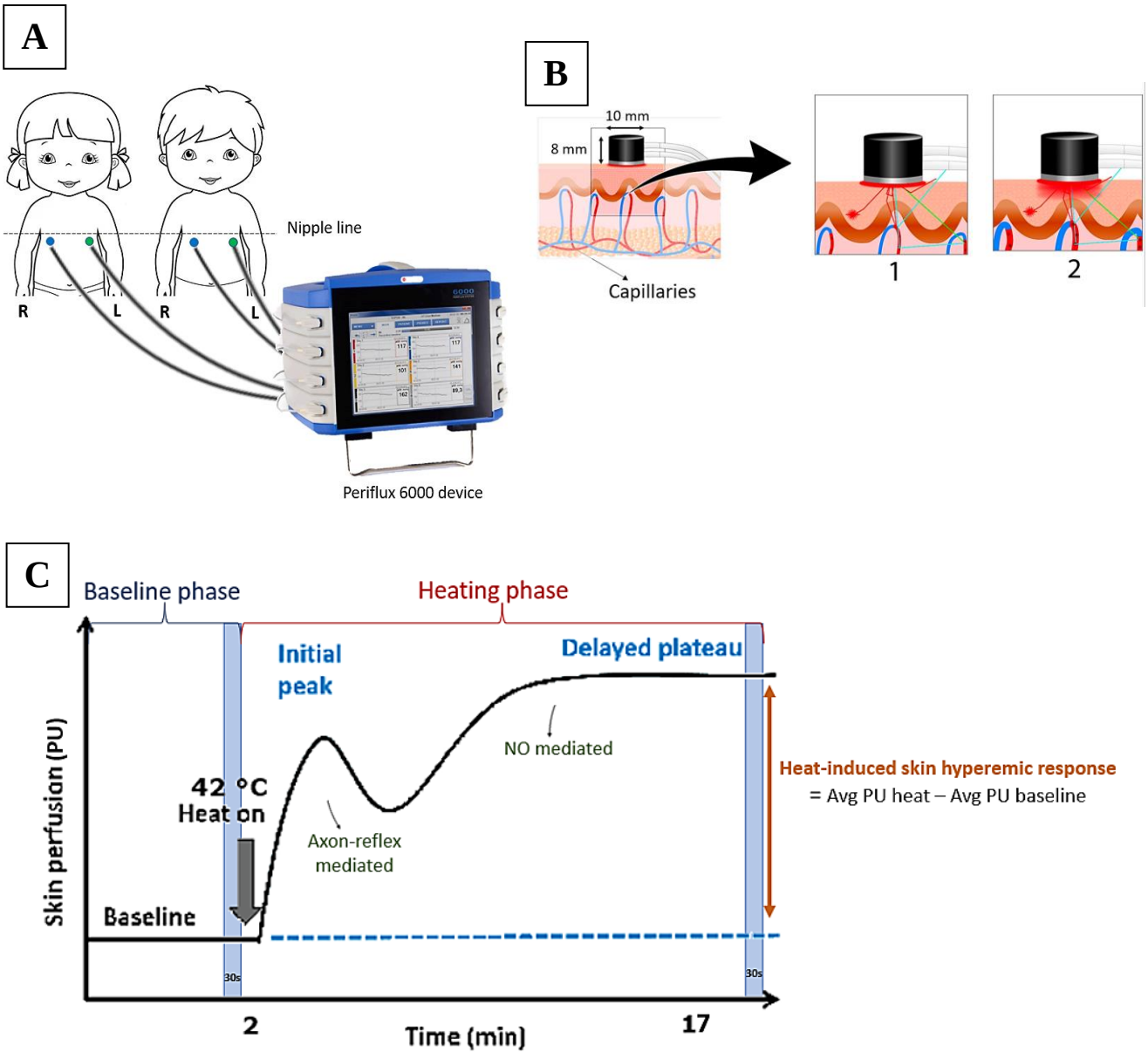

Fig. S6: Skin perfusion measurement. (A) Placement of the laser Doppler probes and the main unit of the Periflux 6000 device. The two thermostatic laser Doppler probes were placed on the child's chest directly under the left and right nipple using double-sided tape. The main unit is operated by a touch screen and shows the measurement data of blood perfusion. **(B) Thermostatic laser Doppler probe (10 by 8 mm) that can simultaneously detect blood flow changes according to the Doppler phenomenon and locally heat the skin.** (1) The probes emit a low-power laser light beam (780 nm) with a known frequency (*i.e.* 32 Hz), which is scattered and partly absorbed by the skin tissue. Light hitting moving red blood cells in the skin vessels changes frequency (Doppler shift), while light hitting static objects is unchanged. The Doppler shift's frequency and size are associated with the velocity and concentration of red blood cells, respectively. The information of the returning light signals is picked up by the probe and converted into an electric signal on the Periflux 6000 device to analyze the blood flow in arbitrary perfusion units (PU). (2) One probe additionally heats the skin locally to 42°C, which induces thermal hyperemia. **(C) Graphic representation of the skin perfusion (PU units) over time (minutes) after thermal provocation.** After a baseline perfusion recording for 2 minutes, the temperature of the right probe was rapidly and locally increased to 42°C for 15 minutes to elicit maximal vasodilation. Skin perfusion shows an initial peak directly after heating, which predominantly relies on the local sensory nerves and nitric oxide (NO), and a secondary peak with a plateau phase predominantly mediated by NO. The heat-induced skin hyperemic response was expressed as the absolute difference of the average perfusion units increase during stabilization in the 15-min heating phase and the average 2-min baseline phase. Average perfusion units were calculated during the last 30 seconds of each phase (indicated by the blue bars).
PU = perfusion units; Avg = average

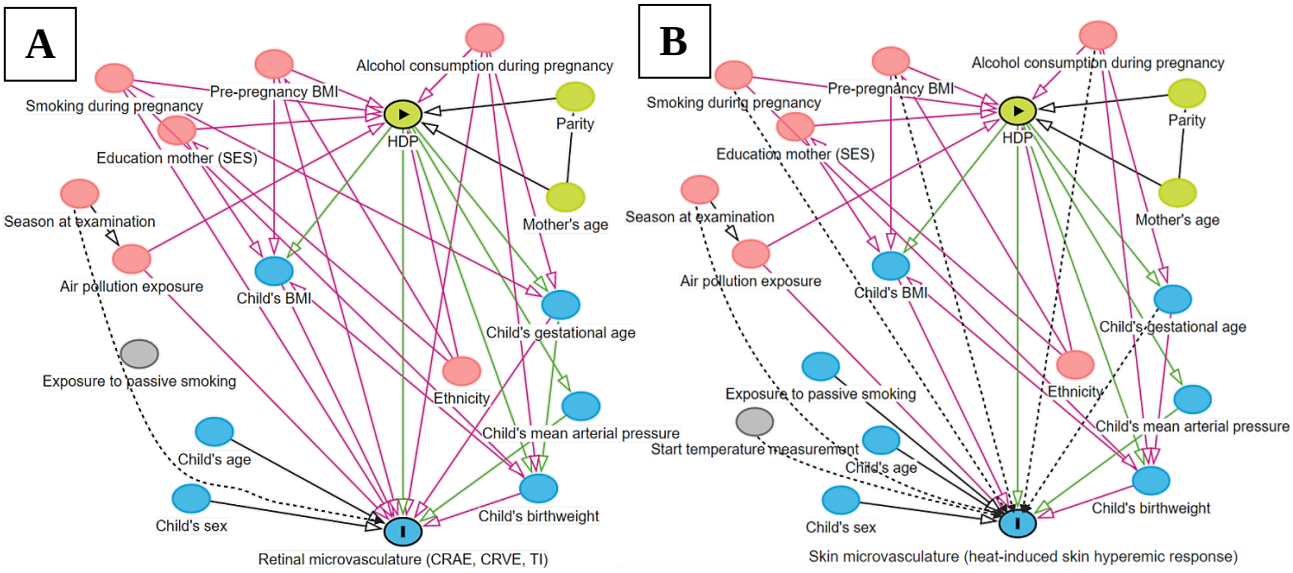

Fig. S7: Directed acyclic graph (DAG) for the retinal (A) and skin microvasculature (B). This graphical representation shows causal relationships between variables (outcome (▌), exposure (►), and covariates). The variables and connections were added based on literature research. Green connections represent possible mediating or causal factors and pink connections represent possible confounding factors that have both effect on the exposure (HDP) and outcome variable (retinal and skin microvasculature). Dotted line connections represent possible effects that are not yet reported/indicated by literature. Black lines show connections of variables that only have an influence on the exposure or outcome. Green spheres represent covariates that have an influence on the exposure variable, blue spheres are covariates influencing the outcome variable. Pink spheres represent possible confounding variables. Grey spheres are variables that had no/no reported influence on the exposure or outcome.
HDP = hypertensive disorders of pregnancy; SES= socio-economic status; BMI = body mass index; CRAE = central retinal arteriolar equivalent; CRVE = central retinal venular equivalent; TI = tortuosity index

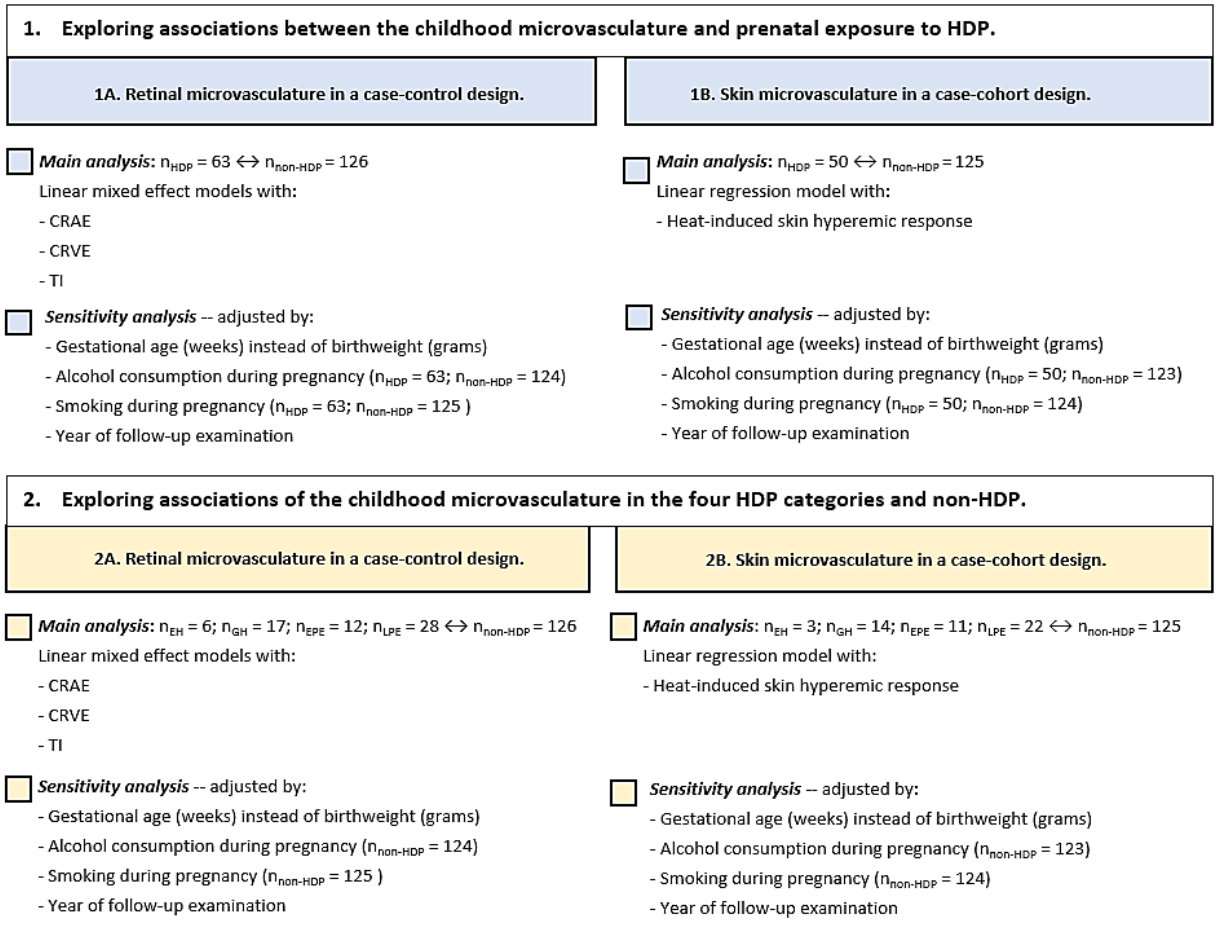

Fig. S8: Flowchart of data analyses. This study had two major purposes: the first one is exploring associations between the childhood microvasculature and prenatal exposure to HDP, by comparing retinal and skin microvascular data of the HDP and non-HDP group in a case-control and case-cohort design, respectively. The second one is exploring associations of the childhood microvasculature in the four categories of HDP and the non-HDP group. This lead to four main analysis with additional sensitivity analyses for gestational age (weeks) instead of birthweight (grams), adjustment of alcohol consumption and smoking during pregnancy, and adjustment for year of follow-up examination.
(non-)HDP = (non-)hypertensive disorders of pregnancy; EH = essential hypertension; GH = gestational hypertension; EPE = early -onset pre-eclampsia; LPE = late-onset pre-eclampsia

Table S1: Characteristics of the entire HDP population (n = 69) compared to entire non-HDP population (n = 549), expressed in mean (SD) or frequency (%). P-values were calculated to compare the two populations.

Characteristic	HDP *N = 69*	Non-HDP *N = 549*	p-value
Mother			
Age at birth child (years)	30.8 (4.21)	30.2 (4.24)	0.22
Pre-pregnancy BMI (kg/m²)	24.9 (4.07)	24.2 (4.36)	0.2
Smoking behavior during pregnancy [a]			0.93
Never smoked	49 (71)	374 (68.1)	
Stopped during pregnancy	14 (20.3)	119 (21.7)	
Smoked during pregnancy	6 (8.7)	51 (9.3)	
Alcohol consumption during pregnancy [a]			0.03
Yes	5 (7.2)	101 (18.4)	
No	64 (92.8)	435 (79.2)	
Education level [a]			0.03
Low (no high school diploma)	5 (7.2)	22 (4)	
Middle (high school diploma)	27 (39.1)	150 (27.3)	
High (college degree or higher)	37 (53.6)	374 (68.1)	
Child			
Sex			0.2
Male	27 (39.1)	265 (48.3)	
Female	42 (60.9)	284 (51.7)	
Age at examination (months)	65.7 (6.93)	55.1 (5.05)	$7.4*10^{-20}$ [b]
Gestational age (weeks)	36.9 (3.81)	39.6 (1.61)	$2.7*10^{-7}$ [b]
Birth weight (grams)	2770 (941)	3410 (503)	$4.7*10^{-7}$ [b]
Ethnicity [a, c]			/
European	34 (49.3)	517 (94.2)	
Non-European	2 (2.9)	29 (5.3)	
MAP (mmHg) [a]	74.3 (7.94)	71.2 (8.86)	0.004
Height at examination (cm) [a]	113 (6.67)	108 (5.15)	$6.7*10^{-9}$ [b]
Weight at examination (kg) [a]	20.5 (3.48)	18.7 (2.57)	$1.2*10^{-4}$ [b]
BMI at examination (kg/m²) [a]	15.9 (1.24)	16.1 (1.29)	0.23
Season at examination			0.03
Spring	24 (34.8)	141 (25.7)	
Summer	21 (30.4)	138 (25.1)	
Autumn	7 (10.1)	140 (25. 5)	
Winter	17 (24.6)	130 (23.7)	

(non-)HDP = (non-)hypertensive disorders of pregnancy; MAP = mean arterial pressure; BMI = body mass index

[a] Data was missing for: smoking behavior during pregnancy ($n_{non\text{-}HDP} = 5$); alcohol consumption during pregnancy ($n_{non\text{-}HDP} = 13$); mother's education level ($n_{non\text{-}HDP} = 3$); ethnicity ($n_{HDP} = 33$ and $n_{non\text{-}HDP} = 3$); MAP ($n_{HDP} = 1$ and $n_{non\text{-}HDP} = 38$); height ($n_{non\text{-}HDP} = 3$); weight ($n_{non\text{-}HDP} = 4$); BMI ($n_{non\text{-}HDP} = 4$).

[b] P-values were obtained with a Welch's t-test instead of an unpaired t-test.

[c] Ethnicity was determined based on the country of origin of the grandparents; European when 2 out of 4 are European, non-European when 3 or more are non-European.

Table S2: Characteristics of the total non-HDP population (n = 549) compared to the optimal pair matched population for the retinal microvasculature (n = 126) and the constrained full matched population for the skin microvasculature (n = 125), expressed in mean (SD) or frequency (%). P-values were calculated to compare the three different populations.

Characteristic	Non-HDP Total N = 549	Non-HDP Retinal microvasculature N = 126	Non-HDP Skin microvasculature N = 125	p-value
Mother				
Age at birth child (years)	30.2 (4.24)	29.8 (4.47)	30.8 (3.88)	0.18
Pre-pregnancy BMI (kg/m²)	24.2 (4.36)	24.6 (4.74)	23.4 (3.45)	0.3 [b]
Education level [a]				0.15
Low (no high school diploma)	22 (4)	7 (5.6)	8 (4.6)	
Middle (high school diploma)	150 (27.3)	34 (27)	41 (23.4)	
High (college degree or higher)	374 (68.1)	85 (67.5)	126 (72)	
Child				
Sex				0.16
Male	265 (48.3)	51 (40.5)	65 (52)	
Female	284 (51.7)	75 (59.5)	60 (48)	
Age at examination (months)	55.1 (5.05)	60.8 (4.71)	57.8 (6.75)	$< 2*10^{-16}$ [b]
Birth weight (grams)	3410 (503)	3380 (467)	3420 (477)	0.8
MAP (mmHg) [a]	71.2 (8.86)	16.2 (1.32)	15.9 (1.3)	0.4 [b]
BMI at examination (kg/m²) [a]	16.1 (1.29)	71.4 (8.72)	69.7 (6.57)	0.43 [b]
Season at examination				$< 2*10^{-16}$
Spring	141 (25.7)	50 (39.7)	87 (69.6)	
Summer	138 (25.1)	20 (15.9)	38 (30.4)	
Autumn	140 (25. 5)	24 (19)	0 (0)	
Winter	130 (23.7)	32 (25.4)	0 (0)	

non-HDP = non-hypertensive disorders of pregnancy; MAP = mean arterial pressure; BMI = body mass index

[a] Data was missing for: mother's education level ($n_{non\text{-}HDP\ total} = 3$); MAP ($n_{non\text{-}HDP\ total} = 38$); BMI ($n_{non\text{-}HDP\ total} = 4$).

[b] P-values were obtained with a Kruskal-Wallis test instead of a one-way ANOVA test.